

UNCLASSIFIED

AD 434301

DEFENSE DOCUMENTATION CENTER

FOR

SCIENTIFIC AND TECHNICAL INFORMATION

CAMERON STATION, ALEXANDRIA, VIRGINIA



UNCLASSIFIED

NOTICE: When government or other drawings, specifications or other data are used for any purpose other than in connection with a definitely related government procurement operation, the U. S. Government thereby incurs no responsibility, nor any obligation whatsoever; and the fact that the Government may have formulated, furnished, or in any way supplied the said drawings, specifications, or other data is not to be regarded by implication or otherwise as in any manner licensing the holder or any other person or corporation, or conveying any rights or permission to manufacture, use or sell any patented invention that may in any way be related thereto.

434301

434301

64-
DASA-1440
USNRDL-TR-706
13 September 1963

HYDRA PROGRAM

HYDRA IIB SERIES - INVESTIGATION BY WATER SAMPLING OF
THE INTERNAL STRUCTURE OF COLUMNS RESULTING FROM
SMALL SHALLOW UNDERWATER EXPLOSIONS

by
K.W. Kaulum

U.S. NAVAL RADIOLOGICAL
DEFENSE LABORATORY

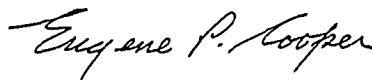
SAN FRANCISCO • CALIFORNIA • 94135

RADIOLOGICAL EFFECTS BRANCH
E.A. Schuert, Head

CHEMICAL TECHNOLOGY DIVISION
L.H. Gevantman, Head

ADMINISTRATIVE INFORMATION

The work reported is part of a project sponsored by the Defense Atomic Support Agency under NWER Program A-7, Subtask 10.002. This project is described in the USNRDL Technical Program Summary for Fiscal Years 1963, 1964 and 1965 dated 1 May 1963 wherein it is identified as Program A-1, Problem 3.



Eugene P. Cooper
Scientific Director

12ND NRDL P1 (9/63)



D.C. Campbell, CAPT USN
Commanding Officer and Director

ABSTRACT

The internal structure of the columns from one-pound high-explosive shallow underwater explosions has been investigated by means of water sampling for several shallow charge depths. Water samples taken at varying times across the column diameter at several heights up to 8 ft are used to compute the thickness of the water seal between the explosion product gas bubble and the air of the initial column formation and the total volume of water ejected into the column. These are compared with computed seal thickness and water volume assuming outward flow of the water over the charge to be only radial in direction. Sampling data is used along with above-and below-surface photographs to construct a time sequence of the column structure for charge depths of 5.5 and 12 in. It is shown that true radial flow of water over the charge occurs only during the very early initial bubble expansion and is soon supplanted by a tangential flow which converges well above the surface. The converging water results in both an upward jet which rises high into the air and a downward jet which penetrates through the underwater bubble.

SUMMARY

The Problem

A complete phenomenology of shallow underwater explosions is unavailable for use in the prediction of the radiological effects from underwater nuclear weapons. Only recently have attempts been made to determine on a small scale some internal features of the resulting above-surface plumes with sampling instruments and pressure gages. This investigation will undertake the problem of describing the internal structure of the columns with time for shallow 1-pound underwater explosions. Sampling at several levels above the water surface provides the basic data for determination of the internal structure.

Findings

It was found that the water forming the column flows from the charge center both radially and tangentially, thus covering well above the water surface. The converging water forms both an upward jet rising high above the surface and a downward jet which protrudes through the expanding underwater bubble. The volume of water flowing into the downward jet is approximately equal to that in the upward jet. The total projected volume of water in the column has been determined with time for charge depths of 5.5 and 12 inches. Thickness of the water seal between the explosion products and the perturbed water surface is given for charge depths of 2.5 to 24 in. Comparison of these values

of seal thickness and volume of water projected into the column with those values calculated by assuming pure radial flow of water surrounding the charge shows that water flow in the column has a large non-radial or tangential component.

PREFACE

The U. S. Naval Radiological Defense Laboratory is conducting the Hydra Program in order to determine the radiological effects from underwater nuclear explosions. The ultimate objective of the program is to analyze and express as functions of yield and depth of burst those radiological effects that can influence fleet and aircraft operations and/or design. The program includes a series of field tests to investigate comparable nuclear phenomena through use of high-explosive charges. This project, Hydra IIB, is one of this series in which experimentation is limited to shallow underwater explosions of one-pound charges.

To satisfy its objectives, the project has several experimental phases: (1) determination of the water motion adjacent to the expanding underwater bubble; (2) determination of the dynamic internal structure of the above-surface column; and (3) determination of the transfer of explosion products from the underwater bubble into the column, and their distribution. Phase 1 will be reported in a report now in preparation.* This report describes the results of phase 2. Experimental work on phase 3 is now in progress.

*R. R. Hammond, K. W. Kaulum. An Investigation of Water Flow Adjacent to Shallow Underwater Explosions Using Fluorescent Dyes and Photographic Techniques, Hydra IIB. Technical report now in preparation at USNRDL.

CONTENTS

ABSTRACT	1
SUMMARY	ii
PREFACE.	iv
CHAPTER 1 INTRODUCTION.	1
Background.	1
Objectives.	3
CHAPTER 2 EXPERIMENTAL DETAILS	4
Experimental Plan.	4
Instrumentation.	5
Test Facilities.	5
Sampling Device.	6
Sampler Calibration.	10
Explosive Charges.	12
Charge Location.	12
Sampler Operation.. . . .	13
CHAPTER 3 RESULTS.	15
Sampling Data.	15
Data Reduction	15
Data Presentation.	16
Carbon in Water Samples.	26
Total Ejected Water.	29
Calculation and Results.	29
CHAPTER 4 ANALYSIS AND DISCUSSION	33
Radial Flow.	33
Radial Flow Equations.	33
Comparison With Experimental Results	36
Total Ejected Water Calculations.	40
Internal Structure.	43
Time Sequence of Column Structure	43
Carbon in Samples.	49
CHAPTER 5 CONCLUSIONS.	51
REFERENCES.	54
APPENDIX	55

TABLES

2.1	11
3.1	Total Ejected Water in Liters	31
4.1	40

FIGURES

2.1	General View of Test Pond and Instrumentation Support Structure With Camera Bay in Foreground.	7
2.2	Sampler Beam in Place With Samplers Installed.	7
2.3	Details of Sampler.	8
3.1	Sample Volume vs Radius at Early Time for 2.5-in. Charge Depth.	18
3.2	Sample Volume vs Radius at Early Time for 5.5-in. Charge Depth (4.5 in. for 0-17 msec).	18
3.3	Sample Volume vs Radius at Early Time for 6.3-in. Charge Depth.	19
3.4	Sample Volume vs Radius at Early Time for 12-in. Charge Depth.	19
3.5	Sample Volume vs Radius at Early Time for 24-in. Charge Depth.	20
3.6	A & B Sample Volume vs Radius for 2.5-in. Charge Depth. .	21
3.7	A & B Sample Volume vs Radius for 5.5-in. Charge Depth. .	22
3.8	A & B Sample Volume vs Radius for 7.5-in. Charge Depth. .	23
3.9	A & B Sample Volume vs Radius for 12-in. Charge Depth. .	24
3.10	A & B Sample Volume vs Radius for 24-in. Charge Depth. .	25
3.11	Total Event Sample Volume vs Radius for 5.5-in. Charge Depth.	27
3.12	Total Event Sample Volume vs Radius for 12-in. Charge Depth.	28
3.13	Total Ejected Water vs Time for 5.5-in. and 12-in. Charge Depths.	32
4.1	Geometry for Radial Flow	34
4.2	Actual and Calculated Sample to Volume vs Radius for 4.5-in. Charge Depth.	37
4.3	Actual and Calculated Seal Thickness vs Charge Depth. .	39
4.4	Actual and Calculated Total Projected Water vs Charge Depth.	42
4.5	Time Sequence of Bubble and Column Internal Structure for 5.5 in. Charge Depth.	45
4.6	Time Sequence of Bubble and Column Internal Structure for 12 in. Charge Depth.	47

CHAPTER 1

INTRODUCTION

Background

Low-yield underwater chemical explosions have been extensively used in the past to simulate the phenomena produced by underwater nuclear detonations.^{1,2,4} The results of these studies have indicated the applicability as well as the limitations of such simulation so that valid work can be accomplished with one-pound charges over a limited range of shallow depths and a limited period of time. These limitations result from the inability to scale gravity, which acts on the system in the form of a buoyant force on the underwater bubble and a deceleration force on the rising column. However, these gravity forces are small compared to other forces acting during the initial bubble-expansion period and consequently can be ignored for charge depths substantially less than the first maximum bubble radius. Snay³ classifies a charge depth of one-half the maximum bubble radius as "shallow" and considers as characteristic of a shallow detonation a strong interaction of the bubble with the water surface during its first expansion.

From these considerations, effects measurements using one-pound charges are useful in simulating larger yields, if detonation depths are limited to one-half the bubble radius, (approximately 2 ft for a one-pound charge), and for times associated with the first bubble-expansion period. The one-pound yield produces above- and below-surface results of optimum size for detailed study with the proper instrumentation and affords obvious advantages over full scale yields.

Water-sampling techniques were used first for investigation of column structure during the Hydra I test series,⁴ conducted in the summer of 1959. The Hydra I work has provided an extensive and most useful documentation of shallow low-yield underwater explosions. However, review of the sampling data revealed two limitations of its use for study of internal column structure. First, all sampling was done at a height of two feet above the water surface. Second, there are indications that the columns were perturbed by the sampling instrumentation.

Investigation of the internal structure of the column has also been attempted by both NRDL and the Naval Ordnance Laboratory,⁵ using a pressure gage suspended over the plume. These measurements indicate the initial column top to be composed of a spray followed by a solid water seal. If a seal velocity is assumed, the seal thickness can be determined from the pressure record. Determination of other internal features of the column such as later convergence and water volumes from pressure records appears very difficult. These empirical experimental efforts have been conducted without benefit of any theory to predict the column structure.

An analytical model to describe the shape of the expanding underwater explosion product bubble and associated early above-surface effects resulting from a shallow underwater explosion was first suggested by C. F. Ksanda. The model is based on the assumption of pure radial flow of water outward from the charge center. Applied to a shallow explosion, it predicts that the water over the charge rapidly moves upward with the same general shape of the observed column, with a thin seal of water bounding the explosion-product gases. The model has been extended by Hammond and Young⁶ who have applied it to a large range of yields including one-pound of TNT. One of the objectives of the first phase of

the Hydra IIB project* was an evaluation of this radial-flow assumption for shallow charge depths by photographically tracking the underwater path of dyes that had been placed near the charge. The results indicate that under these conditions, the radial flow assumption is not valid for flow adjacent to the bubble.

Objectives

The objectives of this phase of the Hydra IIB project are: to determine the dynamic internal structure of the above-surface column resulting from shallow one-pound underwater explosions; and to compare the results with those predicted by the theoretical bubble model whose basic assumption allows only flow in the radial direction, in order to further evaluate the validity of this assumption.

As stated above, the Hydra IIB project also has an additional objective of determining the transfer of explosion products from the bubble into the column and their distribution within the column. It is planned to accomplish this by use of a radioactive tracer within the charges as the next phase of the project. Since the internal structure of the column will affect the distribution of explosion products, provision of the internal column structural information needed to plan this future experimental work can be considered as a supplementary objective.

*R. R. Hammond and K. W. Kaulum, "An Investigation of Water Flow Adjacent to Shallow Underwater Explosions Using Fluorescent Dyes and Photographic Techniques, Hydra IIB", USNRDL-TR, in preparation, unclassified.

CHAPTER 2

EXPERIMENTAL DETAILS

Experimental Plan

Sampling of the columns was accomplished with 15 sampling devices supported rigidly over the water by an instrument-support structure. The structure provided support of the samplers at any height up to 12 ft. The sampling device consisted of a sample reservoir and a normally open valve which could be closed at any predetermined time during the event to terminate sampling.

Charge depths of 2.5, 5.5, 7.5, 12 and 24 in. were selected as adequately covering the shallow depth range and matching specific depths used in previous experimental work with 1-lb pentolite charges.

In order to minimize the number of shots, an exploratory approach was used. At least two shots were fired for each charge depth with samplers 2 ft above the surface. The sampling period was terminated very early so as to include only the water seal over the expanding bubble. These shots served to establish reasonable column symmetry and reproducibility of sampling data. Following this were several shots at the 5.5-in. depth and 2-ft sampling height in which sampling was terminated at a later time until a rough time history of sample volumes was obtained. Then for the same charge depth, shots were fired with sampling heights of 4, 6 and 8 ft, with sampling over the total event to determine gross effects of sampling height. A very significant change in the form of the data appeared between 4 ft and 6 ft and continued unchanged to

8 ft, so the 6 ft sampling height was chosen for additional shots. This process was repeated for the 12-in. charge depth and results were much like those for a charge depth of 5.5-in. Since sampling would be continued in the third phase of Hydra IIB, the other charge depths were given minimum coverage in this study.

Instrumentation

Test Facilities

All shots of this test series were conducted at the NRDL test-pond facility located at Camp Parks. The facility consists of a fresh water pond with its associated filter system, a movable instrumentation-support structure, a portable house used as a work shop and office, and an instrumentation van. A general view of the facility is shown in Fig. 2.1.

The pond has the shape of an 18-ft radius hemisphere with a 6-ft wide underwater camera bay extending 10 ft to the south. The pond is constructed of a 12-in.-thick reinforced concrete shell which will withstand detonation of 1-lb HE charges underwater to a depth of approximately 6 ft. The pond contains 90,000 gallons of fresh water at normal operating level. The water is continuously filtered through a 3-unit sand-bed fixed-filter system with a capacity of 100 gpm. When rapid removal of explosion products is desired, an additional diatomaceous-earth filter system with a capacity of 400 gpm is used as well.

An underwater shock-resistant camera housing with adjustable support from above the surface is normally located in the camera bay. This arrangement allows a camera stand-off from the pond center of 25 ft so that wide-angle lenses with little distortion can be used.

The instrument-support structure provides for rigid positioning of instruments over the water surface at any height up to 12 ft. The fabricated steel structure spans the pond and is supported on wheels, facilitating movement away from the pond. A 12 x 12-ft frame within the upright rails can be raised by electric hoists to any height up to 12 ft above the water level and securely locked in place with pins at 6-in. intervals. This frame supports the sampler beam over the center of the pond in a north-south orientation. The streamlined sampler beam supports 15 complete sampling devices. It also protects the sampling devices and their associated wiring from the high-velocity water of the plume. Figure 2.2 shows the sampler beam in place with its cover open and the samplers installed.

Sampling Device

Hydra I sampling results indicated that the large grid of sampling devices might have distorted the normal formation of the column and that samplers were probably biased by spray ricocheting from adjacent supporting structures. To avoid these possibilities, the sampling stations were minimized to a 6-in. spacing along a single diameter across the column. The samplers were placed inside the sampler beam with their snouts extending 8 in. below the sampler beam.

The sampler consists of a snout through which the water sample enters, a normally open valve and a sampler reservoir. It has a straight 3/4-in. bore through to the reservoir cap where the water impinges on a cone and is directed into the annular reservoir. The cap is also provided with ten 1/4-in. vent holes to relieve any pressure build-up within the reservoir. Figure 2.3 is a sectional view of the entire sampler.

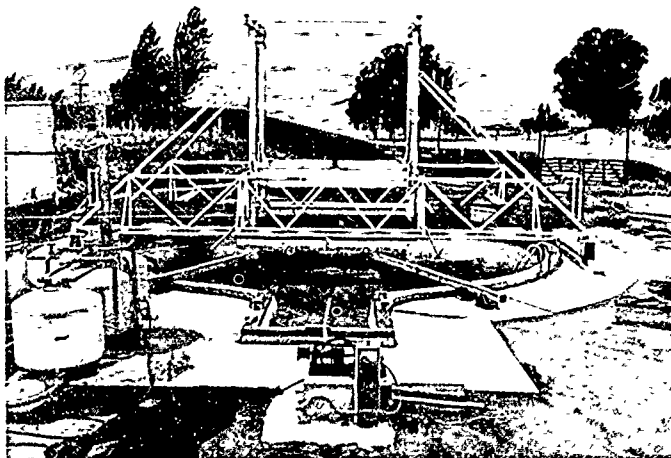


Fig. 2.1 General View of Test Pond and Instrumentation Support Structure With Camera Bay in Foreground

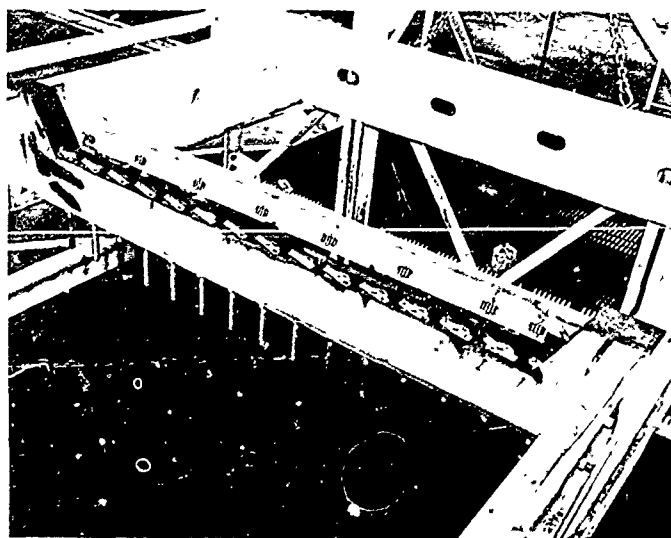


Fig. 2.2 Sampler Beam in Place With Samplers Installed

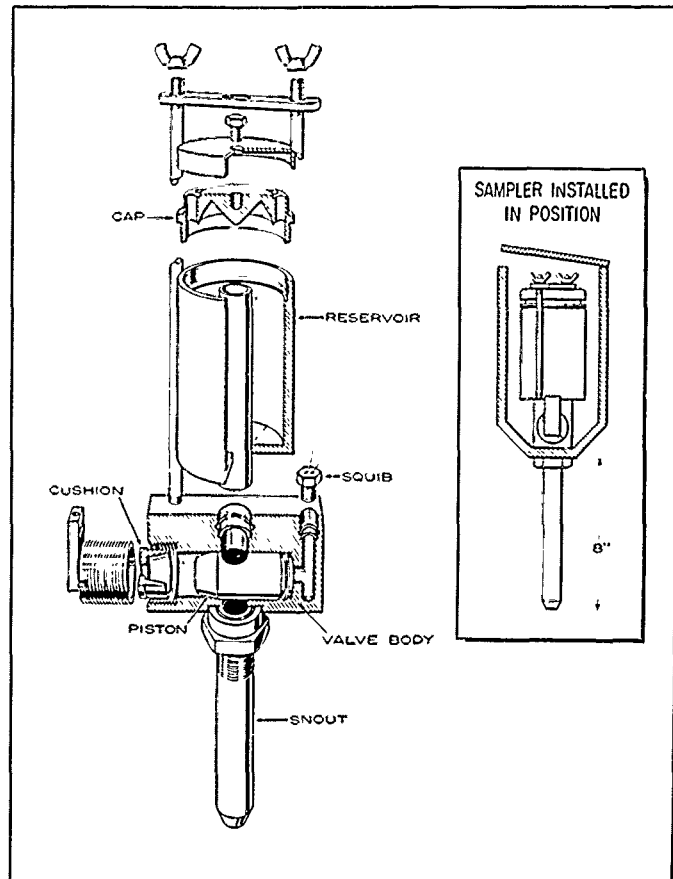


Fig. 2.3 Details of Sampler

The Hydra I sampling device employed a two-stage valve which allowed the device to be opened at any desired time during the event and then closed after a specified sampling period. This arrangement is not practical when a snout extends below the sampler valve because the snout may well contain a sample from early in the event when it is opened later in the event. With this consideration, the sampler was designed with a single-stage normally open valve, consequently sampling is continuous until terminated by closure of the valve at the desired time. This cumulative arrangement requires subtraction of sample volumes from successive shots that have different valve-closing times in order to obtain sample volumes for specific intervals of the event. The same sampler was used to obtain total-event samples by simply not closing the valve during the event.

The valve section of the sampler is required to block flow into the reservoir at a precise predetermined time during the event. This is accomplished by movement of the piston along its horizontal axis to the closed position. The piston is actuated by an electrically initiated explosive squib or gas generator and stopped by a tapered brass cushion which expands slightly to adsorb the piston's energy. The closing time of the valve was determined by means of a light source and phototube. Output of the phototube was recorded on an oscilloscope with its sweep triggered by the same voltage pulse used to detonate the valve squib. Photographing the oscilloscope trace provided an accurate time history of the valve closure. All valves were calibrated when new and several were recalibrated after considerable use. Time required from electrical initiation of the squib to 10 % closure of the valve averaged 2.0 msec, with all values ranging between 1.7 and 2.2 msec. Actual closing time was taken as the time to go from 10 % to 90 % closed, and the average time was 0.86 msec, with a range of 0.6 to 1.1 msec. The standard squib used contained 60 mg of BULLSEYE pistol powder. After five to seven

valve operations, the piston stop cushion apparently work-hardens, allowing the piston to bounce back and the valve to open momentarily. The valve never opens again more than 10 %, and always recloses in 1 msec or less. The overall time for valve closure averages 2.9 msec and could extend to 3.9 msec if piston bounce occurs.

The timing system for valve firing provides triggering voltages to the valve squibs at precise ordered time intervals after shot zero time. Five selectable times from 0-900 msec are available. Briefly, the system consists of an electronic counter-timer unit with the output of four decades switched into diode logic units. Outputs of the logic units trigger thyratrons that allow capacitors to discharge through the squibs. A 10-channel event programmer provides contact closures for starting cameras, recorders, and finally the counter timer for the precision timing system.

Sampler Calibration

The sampler was calibrated in the NRDL high-velocity spray facility,* where bulk density and velocity of spray are known, to determine its effective sampling area. The sampler snout was designed with its leading edge beveled back so as to leave a minimum of flat edge normal to the water path, making its effective area the same as the area of the inside bore. The calibration procedure consisted of locating the sampler in the spray at a position of known bulk density and velocity, exposing it to the spray for several different time periods, and plotting the resulting volumes against time. The sampler was calibrated at a bulk spray density of 0.62 % water at an average velocity of 240 ft/sec. Its effective area is the same as its bore area but only up to a total sample volume of 150 ml after which the effective area decreases. Here the effective area results when the product of spray bulk density, velocity

*T. F. Cochran, Calibration of a High-Pressure Spray Facility, USNRDL-TM-135, dated January 1963.

and orifice area is equated to the sample volume collected per unit time. This sample volume is determined from the plot of volume against time. Since the reservoir has a total volume of 450 ml, the decrease in effective area probably resulted from a partial loss of the sample through the vent holes as the reservoir filled up. To allow use of the sampler when total sample volume was expected to exceed 150 ml, a 3/8-in. bore orifice was provided which slipped into the end of the standard 3/4-in. diameter bore snout. Calibration of this 3/8-in. orifice showed it to have an effective area of 0.195 of the standard snout.

It is apparent that except for the center position, the sample most likely will not enter on a path normal to the orifice. To determine the effect of non-axial sample approach on the effective orifice, calibrations were made with the sampler stem tilted 10° , 30° and 45° to the calibration spray vertical axis. The results are shown in Table 2.1 in terms of flow rates which are directly proportional to effective area.

TABLE 2.1

Approach Angle, θ ($^\circ$)	Measured Flow Rate (ml/sec)	Predicted Flow Rate ($A \cos \theta$) (ml/sec)	Error (%)
0	138	138	-
10	120	136	-12
30	110	119	- 7.5
45	85	97	-12.5

With the expected geometrical reduction of orifice area, the predicted flow rate is $A \cos \theta$ where A is the effective area at $\theta = 0^\circ$ and θ is the angle between the sample orifice axis and the vertical spray axis.

The maximum error is seen to be a reduction of approximately 12 % over that predicted by geometric reduction of the orifice area. Thus it can be concluded that the effective area of the sampler can very nearly be described by $A \cos \theta$ for non axial approach. It was also found that the effective area remained constant up to a total sample volume of 250 ml for $\theta = 10^\circ, 30^\circ, 45^\circ$. No tests were made with non axial approach angle on the 3/8-in. orifice insert.

Explosive Charges

All charges used were 3-1/4-in. diameter bare spheres of 50/50 pentolite with a cylindrical hole to accommodate an Engineer's Special electric detonator. The detonator hole was drilled to a depth that allowed detonation to occur at the charge center. The charges were supported by a lucite ring with a diameter smaller than the charge and were held in place on the ring with a single wrap of electrical tape. The ring was supported by cords to a horizontal tension system. Both are seen below the sampler beam in Fig. 2.2.

All charges were electrically detonated by the thyatron controlled discharge of a 20 μ fd capacitor charged to 1800 volts. This arrangement insured reproducibility of zero time within 15 μ sec.

Test Procedures

Charge Location

Since radial symmetry was assumed for the underwater bubble and column, it was important that the explosive charge be located exactly under the center sampler. The charge support ring was centered by adjustment of the charge support guides with the aid of a plumbbob

supported from the center sampler snout. The charge-support system was arranged so that once its guides were positioned, it could be raised or lowered with no effect on horizontal position.

Accurate setting of charge depth was difficult due to the variable tension on the horizontal charge support with depth. The first procedure used was to set the charge at the water surface and then lower the whole support to the desired depth. However, direct measurement proved this practice to result in a depth setting which was approximately 1-1/8-in. shallower than desired. This accounts for several of the early shots not being positioned at the standard charge depths. The most satisfactory procedure was to lower the charge until its top was just breaking the water surface, and then to lower the support to the desired depth minus one charge radius (1-5/8-in.). Direct measurements showed this method to result in a charge-depth accuracy of within $\pm 1/8$ in. for the 2.5-in. depth and within $\pm 1/2$ in. at the 24-in. depth.

The charge detonator was consistently oriented with its axis horizontal and normal to the sampler-support beam as to minimize its effect on symmetry.

Sampler Operation

Considering the number of combinations of experimental variables required to cover adequately a reasonable number of charge depths, sampling heights and sampling times, it was necessary to limit the number of shots for each specific condition. This required absolute confidence in the reliability and accuracy of the sampling-valve performance with regard to closing as programmed. To insure that the entire system performed as required, many tests were conducted with a detonator instead of an explosive charge and with the timer slowed enough to allow each sampler closure to be separately observed and compared with the programmed

time. As a continuing system check, one of the unused squib-firing channels of each time bank was recorded on an oscillograph along with the zero time for each shot.

The integrity of the samplers after valve closure was tested by firing a shot with all valves closed from the previous shot but with all samples removed and the reservoirs dry. Results were very good. Not a drop of water was found in any of the sampler reservoirs.

CHAPTER 3

RESULTS

Sampling Data

Data Reduction

The three important experimental variables are charge depth, sampling height and sampling time. The charge depths 2.5, 5.5, 7.5, 12.0 and 24 in. were chosen to cover a depth range as discussed in Chapter 1. Sampling height was mostly limited to nominal heights of 2 and 6 ft above the water surface (actual heights were 20-1/2 and 68-1/2 in. to sampler orifice). An adequate time history required as many as eight sampling termination times for each combination of charge depth and sampling height.

In order to reasonably limit the total number of shots required, only two charge depths, 5.5 and 12 in. were investigated intensively with time, while the remaining were covered with three sample termination times: early during the first bubble expansion; at 300 msec; and total event. Even with these limitations, the number of shots for each combination of variables was held to one or two. Three shots were fired if results were badly inconsistent. A single shot was considered acceptable if the sample volumes were equal or greater than those of a shot at an earlier termination time and less than those of a shot at a later termination time. Each shot resulted in two samples for each sampling radius (right and left side), and one for the center.

With only a few (one to six) samples for each specific shot condition, no conventional statistical methods could be applied to the data. The method used consisted of first arithmetically averaging the sample volumes (samples taken with 3/8-in. orifice were corrected to the standard sampler orifice) for each condition and termination time. Next, the average volume for the shortest sampling time was compared with the average volume of the next longer time to see whether a significant increase in volume was evident. Generally, a 20 % increase in average volume was considered significant; but in cases where the average volume for the longer time showed less than a 20 % increase, sample volumes for both times were averaged together and assigned to the earlier time period. This assumes that no significant additional sample was collected during the extended time period. This averaging process was continued for successively longer sampling times until a 20 % increase occurred and a new average volume was established. The aim of this process was to divide the total event sample volume for each sampling radius into its appropriate time intervals during which collection actually took place while utilizing all possible data for the average volume collected in each time interval.

Data Presentation

The results are presented as plots of standard sampler volume vs sampling radius from the column center for each sampling height with coded areas to indicate time intervals. Sample volume is presented both as milliliters per standard sampler and volume per unit area in milliliters per square inch, which are directly related by the effective area of the 3/4-in. bore standard sampler for axial sample flow. Tabulated data used in all plots is given in the appendix, along with the number of samples averaged for each condition, the largest and smallest sample volume and any remarks concerning deletion of a sample or use of the 3/8-in. orifice.

The detailed sampling data is presented in two series of plots for convenience. The first, at the 2-ft sampling height (h_s) and very early in event time, is concerned with the initial column growth resulting from the first expansion of the underwater bubble. These plots of sample volume vs sampling radius for each of the standard charge depths are given in Figs. 3.1 to 3.5. The maximum event time included is 100 msec. In Fig. 3.2, where four time intervals are presented between 0 and 100 msec, sample volume is plotted in cumulative manner with time intervals indicated to show the distribution of sample volume with time. The early sample-volume plots for the other standard charge depths, Fig. 3.1, 3.3, 3.4 and 3.5, are given for only one or two time intervals.

The second series of sampling plots, Fig. 3.6 to 3.10 is concerned with presenting the results at the 2-ft and 6-ft sampling heights for the remaining event time. Part A of each figure gives the sampling volume for the 2-ft sampling height, starting at the latest time previously presented in Figs. 3.1-3.5 and continuing to the end or total event. Each coded area represents a time interval ΔT of the event, with its upper boundary showing the total sample volume from zero time through that interval. The time from the last sample termination to the end of the event is indicated as the "last time +". For example, $T = 700 +$ msec.

Part B of Figs. 3.6 to 3.10 present the sampling volume for the 6-ft nominal sampling height starting at a minimum termination time of 100 msec and continuing throughout the total event. In Fig. 3.6, the sample volumes from the 0-300 msec time interval were averaged with the total-event sample volumes because they were not significantly different. The sample volumes for the 2 ft and 6 ft sampling heights (A and B of each figure respectively) are plotted to the same scale to show the drastic difference in the distributions between the 2 ft and 6 ft heights.

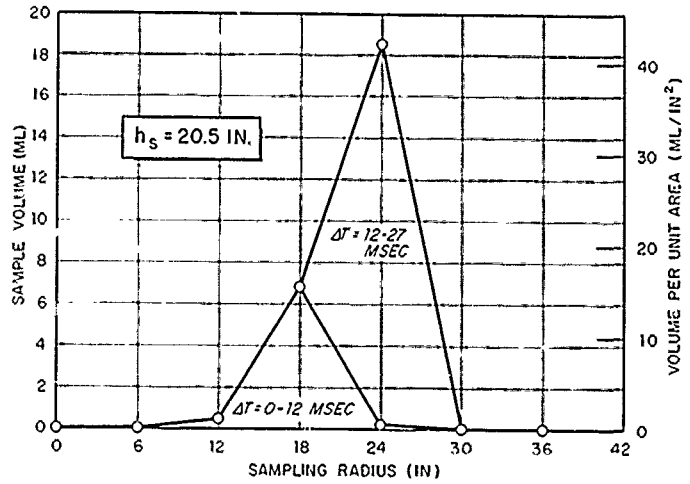


Fig. 3.1 Sample Volume vs Radius at Early Time for 2.5-in. Charge Depth

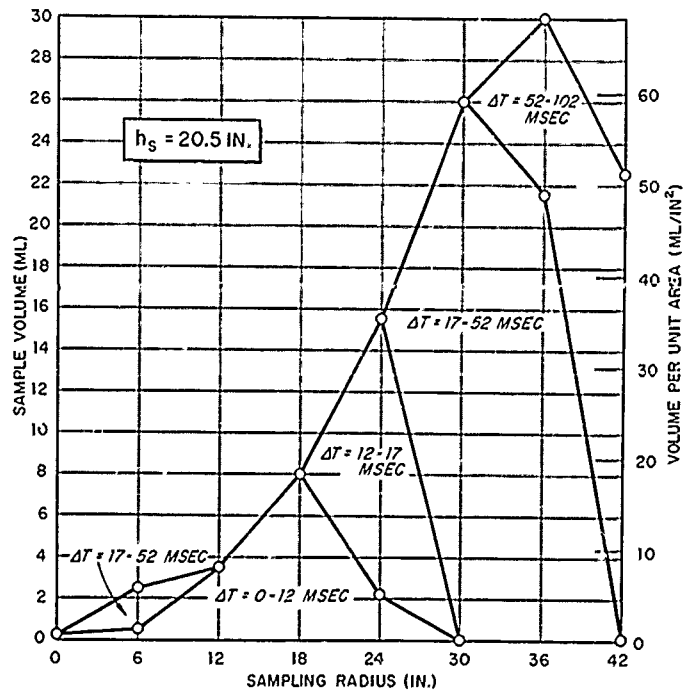


Fig. 3.2 Sample Volume vs Radius at Early Time for 5.5-in. Charge Depth (4.5 in. for 0-17 msec)

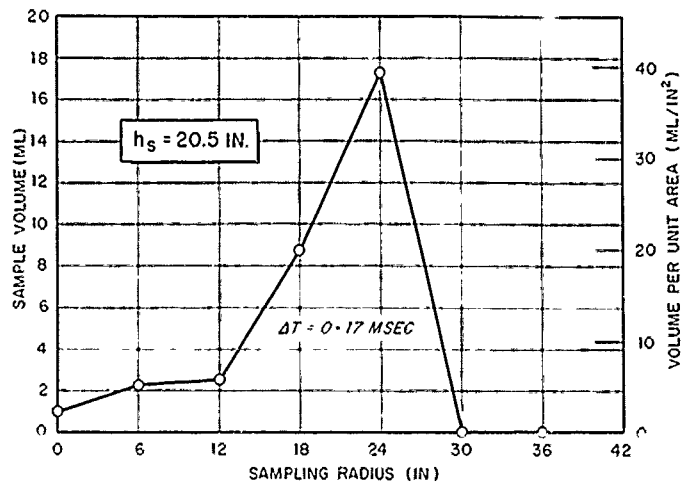


Fig. 3.3 Sample Volume vs Radius at Early Time for 6.3-in. Charge Depth

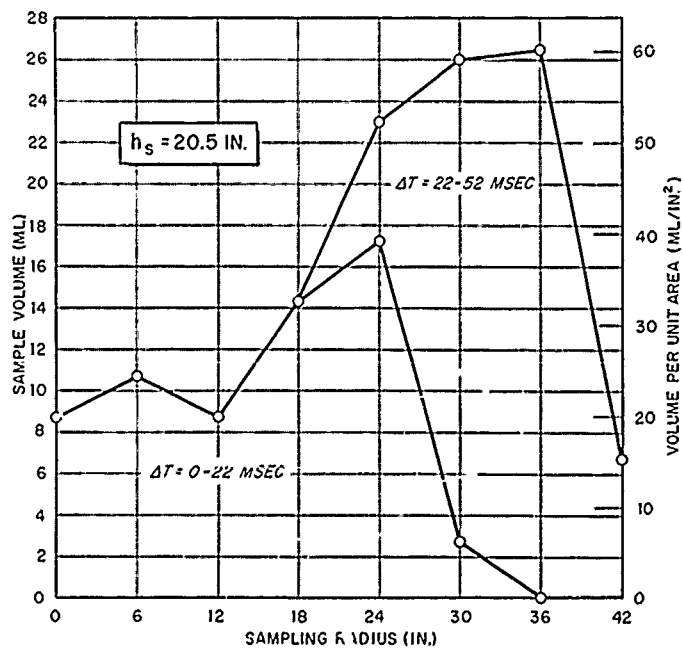


Fig. 3.4 Sample Volume vs Radius at Early Time for 12-in. Charge Depth

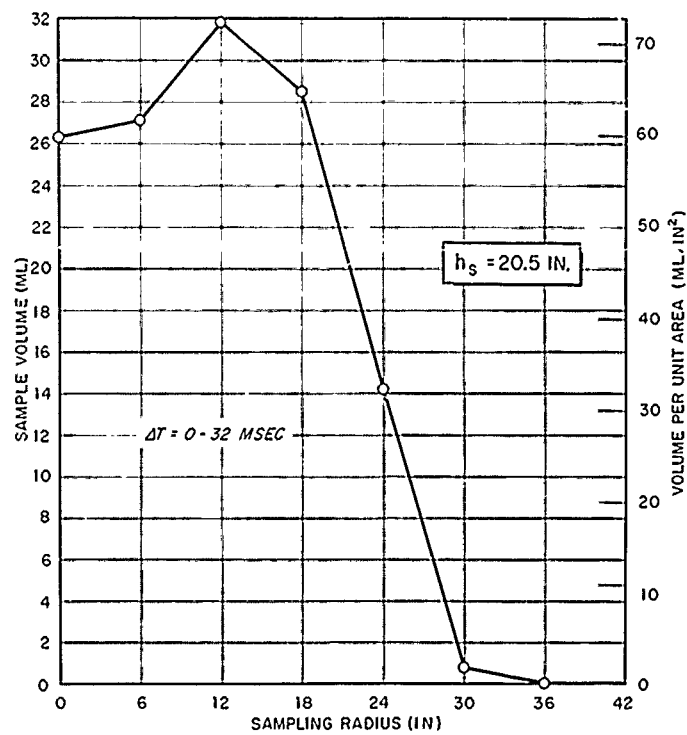


Fig. 3.5 Sample Volume vs Radius at Early Time for 24-in. Charge Depth

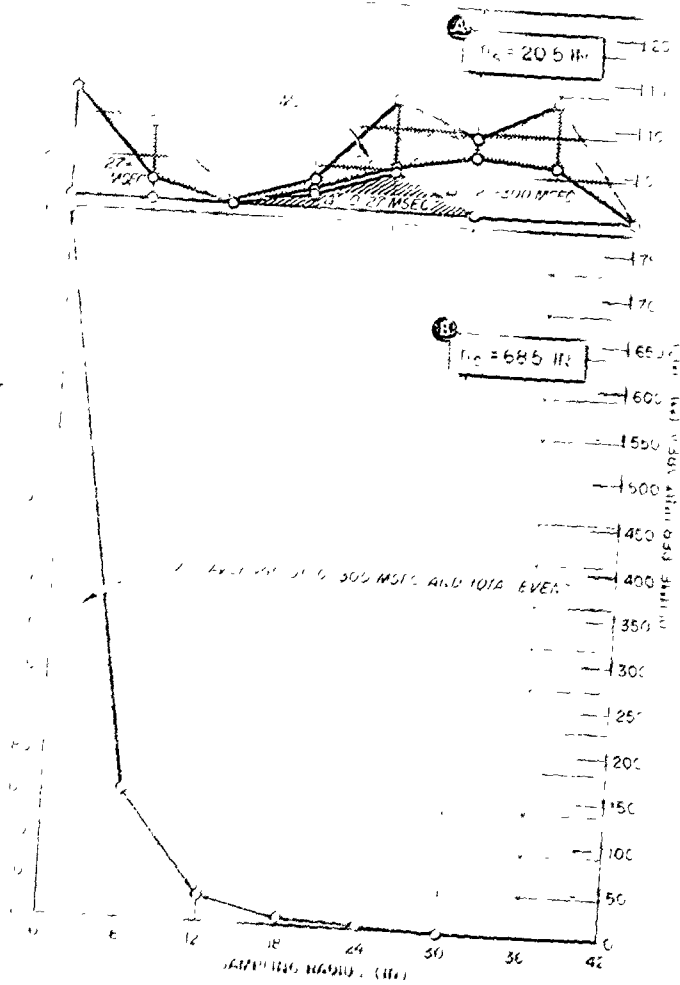


FIG. 3.6 A & B Sample Volume vs. Radius for 2.5-in. Charge Depth

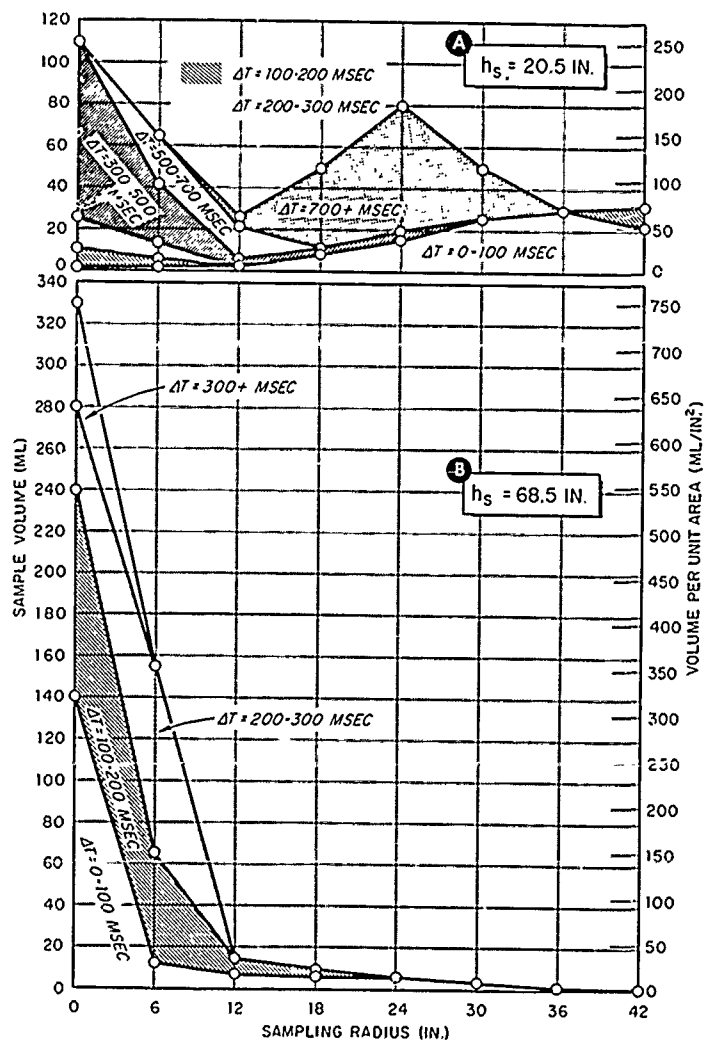


Fig. 3.7 A & B Sample Volume vs Radius for 5.5-in. Charge Depth

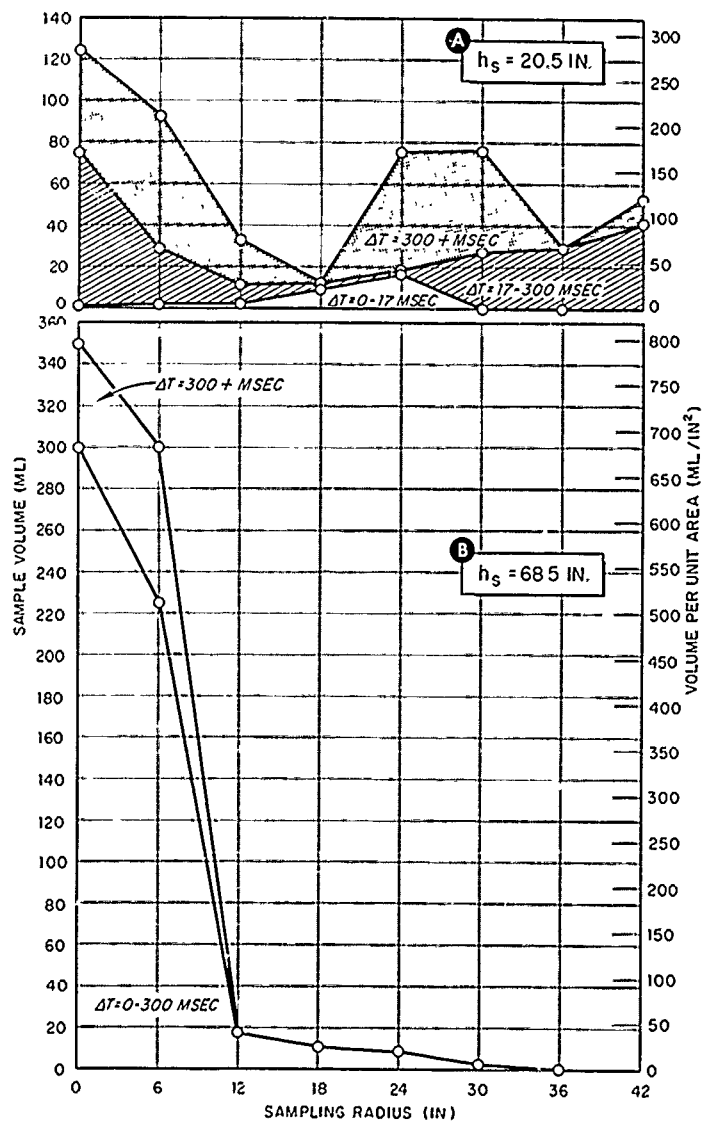


Fig. 3.8 A & B Sample Volume vs Radius for 7.5-in. Charge Depth

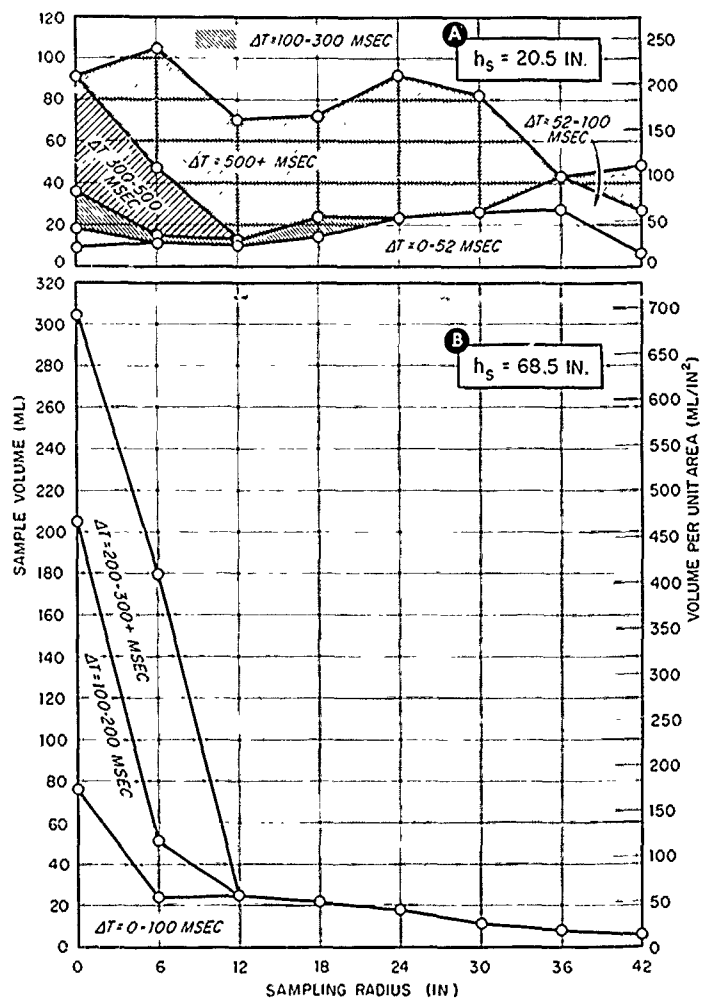


Fig. 3.9 A & B Sample Volume vs Radius for 12-in. Charge Depth

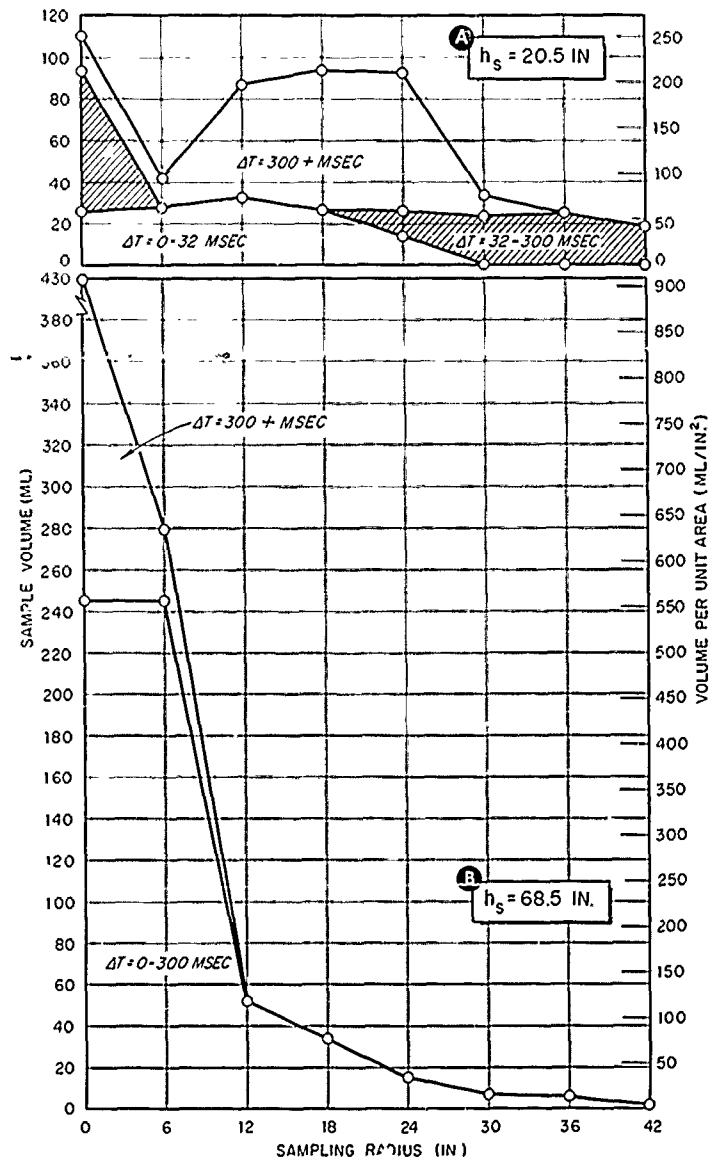


Fig. 3.10 A & B Sample Volume vs Radius for 24-in. Charge Depth

Total event sample volumes (resulting when sampling is not terminated during the event) were taken for several sampling heights at charge depths of 5.5 and 12 in. These plots are given in Figs. 3.11 and 3.12. In Fig. 3.11 it is seen that the sample volume for sampling heights of 6 and 8 ft are very nearly identical at all radii. Also it should be noted that the consistently larger sample volumes for sampling heights of 2 ft with respect to 4 ft observed in Fig. 3.12 result because the volume of water thrown up during the final bubble-venting late in the event does not reach the 4 ft sampling level.

Carbon in Water Samples

The explosion products of pentolite contain a considerable amount of fine particulate carbon which is often present in the column water samples. This offers a possible crude means of tracing the transfer of explosion products to the column. No attempt was made to determine quantitative or relative amounts of carbon in water samples. The presence of carbon was merely observed while the sample volume data was recorded. Considering the cumulative method of sampling, it is possible to determine only the earliest arrival time for the carbon at any specific sampling radius and height.

The results may be summarized as follows:

(a) At the 2-ft sampling height, carbon was present in samples at sample radii of 0, 6 and 12 in. at the earliest sample termination times for all charge depths except 24 in. For the 2.5-in. charge depth, carbon was found in the sampler caps but no water.

(b) At the 6-ft sampling height, carbon was present at sample radii of 0, 6 and 12 in. for all charge depths except 24 in. For the 5.5- and 12-in. charge depths, it appeared in the earliest time interval (0-100 msec)

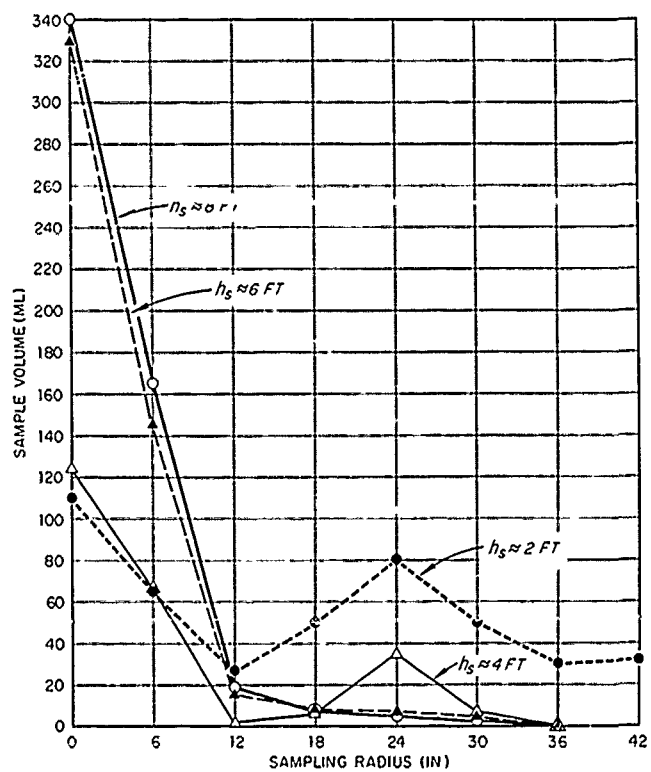


Fig. 3.11 Total Event Sample Volume vs Radius for 5.5-in. Charge Depth

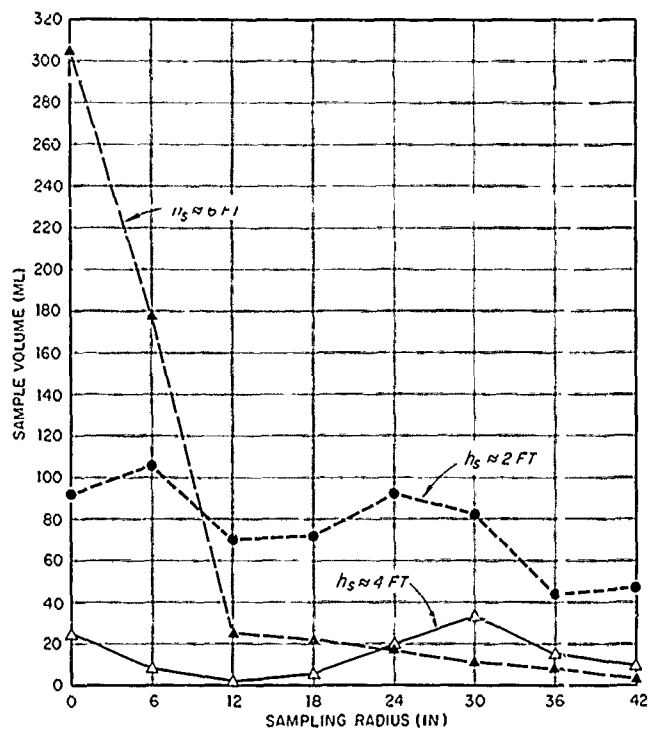


Fig. 3.12 Total Event Sample Volume vs Radius for 12-in. Charge Depth

Also carbon appeared in samples at radii of 18 and 24 in. after 100 msec at 2.5- and 5.5-in. charge depths.

(c) At the one shot with an 8 ft sampling height at charge depth of 5.5 in., carbon was apparent for total-event samples at radii from 6 to 24 in.

It should be made clear that the above observations are to be taken as positive evidence only; i.e., carbon was present if so stated, but not necessarily absent if none was indicated. This results because with no quantitative measurements, judgment as to the presence of carbon in a sample was subject to factors such as dilution and background level of carbon in pond water from previous shots.

Total Ejected Water

Calculation and Results

Calculation of the total ejected water to pass a specific sampling height requires the assumptions (1) that the column is symmetrical about a vertical axis through the charge and the zero-radius samplers and (2) the averaged sample volume for a specific radius, height, and charge depth is an accurate representation of the true volume. Since sample stations were located at 6-in. intervals radially, the horizontal section of the column is divided for calculation into a 3-in. radius circle and seven concentric rings, each having a center radius corresponding to the radius of successive sample stations, and a width of 6-in.

The areas of the center circle and the rings are computed and then divided by the effective area (described under the section on sampling device, Chapter 2) of the standard sampler to give a multiplication factor for each sample radius. The products of the multiplication

factor and sample volume for each sample radius are summed to give the total ejected water volume for a specific charge depth, sampling height, and time interval. No corrections have been made for non-axial approach angles to the sampler orifice because the actual approach angles of the water during the event is unknown.

The results of these calculations for all the available conditions are presented in Table 3.1 where the cumulative volume (in liters) is given for all sampling-termination times when data was taken.

It is evident from Table 3.1 that for any charge depth and sampling time, the ejected water volume at the 2 ft sampling height always exceeds that of any higher sampling level. For charge depths where the greatest range of sampling heights is available for the total event, it can be seen that the volume of ejected water is nearly constant for a sampling height of 4 ft and above. For the 5.5-in. charge depth, the ejected water volume increases about 6 % from a sample height of 4 to 8 ft. For the 12-in. charge depth, a similar increase of 20 % occurs from a sample height of 4 to 6 ft. Quite obviously no additional source of water is available between sampling heights, so the ejected water volume may not increase with successive levels; thus the increase in volume must be considered as minimum possible error in the results.

Total ejected water volume data from Table 3.1 are plotted against time in Fig. 3.13 for charge depths of 5.5 and 12 in. at sampling heights of both 2 and 6 ft. At the 2-ft sampling height, the ejected water volume is seen to increase abruptly until it reaches 100 msec while the volume of the 6 ft sampling height rises more slowly to a maximum at 300 msec. Note that no further flow occurs at the 6-ft sampling level. Figure 3.13 also clearly shows that for the major portion of the event, the total ejected water volume at the 2-ft sampling height is approximately twice

TABLE 3.1
Total Ejected Water in Liters

Charge Depth (in.)	Sampling Height (in.)	Termination of Sampling (Milliseconds)											Total Event
		12	17	22	27	32	52	100	200	300	500	700	
2.5	20.5 68.5	11.3	47.2		52.0				214 78			431 78	
5.5	20.5 44.5 68.5 92.5		48.0*			183	297	323	328	364	392	644 145 149 153	
7.5	30.5 68.5		51.8**						419 195			600 236	
12.0	20.5 44.5 68.5			80.5***		257	384		405	425		947 230 271	
24.0	20.5 68.5						178	200	271			678 396	
						122			354 314				

* Actual charge depth = 4.5 in.

** Actual charge depth = 6.5 in.

*** Actual charge depth = 10.75 in.

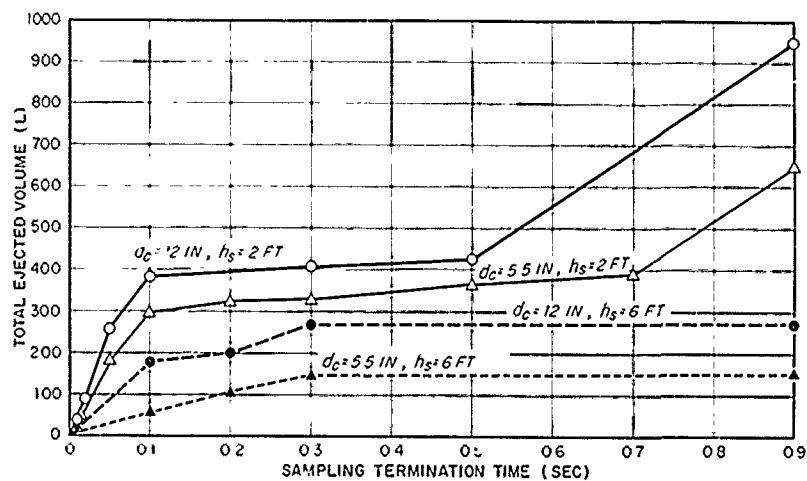


Fig. 3.13 Total Ejected Water vs Time for
5.5-in. and 12-in. Charge Depths

that at the 6-ft sampling level. The volumes for total event have been plotted at 0.9 sec because films show this to be approximately the time at which all upward motion of water has ceased.

CHAPTER 4

ANALYSIS AND DISCUSSION

Radial Flow

Radial Flow Equations

As previously indicated, an objective of this report is to compare experimental results with those predicted assuming radial flow of water about the charge. The thickness of the water seal for the first bubble expansion and the resulting sample volumes expected may be calculated if pure radial flow is assumed as in Reference 6. A general expression for seal thickness at any sample height (h_s), charge depth (d_c) and sampling radius described by the angle θ is derived as follows. From Fig. 4.1 it can be seen that if volume is conserved, the projected volume at a sampling location described by θ and r_2 is

$$A_{r_2} t = V_{r_1} - V_{r_0} \quad (1)$$

where A_{r_2} is the area of the base of the pyramidal element at radius r_2 , t is the seal thickness and $V_{r_1} - V_{r_0}$ is the volume of water in the element between the charge and the water surface before the expansion. The angle θ should be limited to less than 60° . The volume of pyramidal element is:

$$V = 1/3 A_r r$$

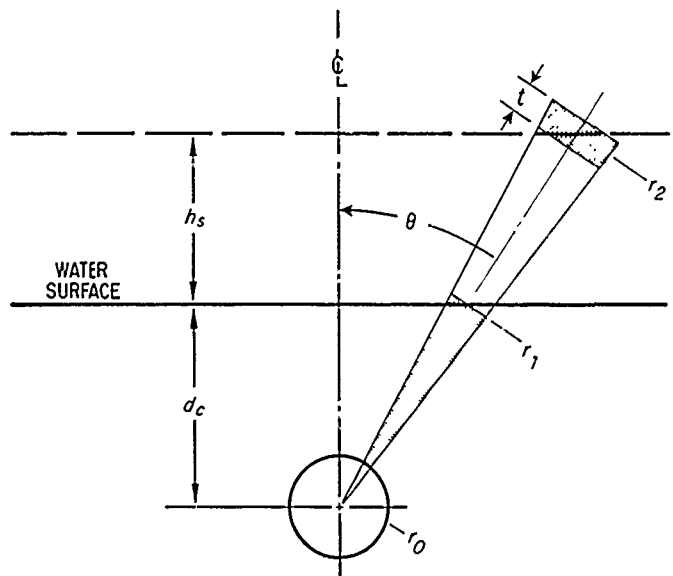


Fig. 4.1 Geometry for Radial Flow

and the base area A_r is proportional to the radius squared so Eq. 1 can be written

$$r_2^2 t = 1/3 r_1^3 - 1/3 r_0^3 \quad (2)$$

or

$$t = \frac{r_1^3 - r_0^3}{3 r_2^2} \quad (3)$$

From Fig. 4.1

$$r_1 = \frac{d_c}{\cos \theta}, \quad r_2 = \frac{d_c + h_s}{\cos \theta}$$

and r_0 is the charge radius. Substituting in Eq. 3, the seal thickness for any charge depth and sampling location is given by

$$t = \frac{(d_c / \cos \theta)^3 - r_0^3}{3(d_c + h_s / \cos \theta)^2} \quad (4)$$

and for $\theta = 0^\circ$, the seal thickness on the center axis is

$$t_0 = \frac{d_c^3 - r_0^3}{3(d_c + h_s)^2} \quad (5)$$

The volume collected by a sampler with its axis normal to the original water surface as the seal passes is

$$V = tA \cos \theta$$

where t is the seal thickness given by Eq. 4, and A is the effective sampler area for axial flow. The simple geometrical reduction of sample volume by $\cos \theta$ is considered to be the minimum reduction expected due to non-axial approach angle of the water seal to the sampler orifice. Any

energy lost by the sample entering the orifice such as impaction on the stem wall must result in a net reduction of velocity since all of the sample's hydrodynamic energy is originally associated with its velocity. The reduction of velocity within the sampler, below that of the approaching water, can only result in an inefficient process and reduced sample volume. Sampler calibration test results are presented under the section, Sampling Device, Chapter 2, that support the above conclusions.

Substituting the expression for t from Eq. 4, we have

$$V = A \cos \theta \frac{(d_c / \cos \theta)^3 - r_o^3}{3(d_c + h_s / \cos \theta)^2} \quad (6)$$

which can be reduced to

$$V = A \frac{d_c^3 - (r_o \cos \theta)^3}{3(d_c + h_s)^2} \quad (7)$$

Examination of Eq. 7 reveals that the sample volume is independent of the angle θ with the exception of the term $(r_o \cos \theta)^3$. Its effect is seen to be negligible unless the charge depth d_c approaches the charge radius r_o . For depths of interest, the sample volume should be constant across the column diameter for a specific charge depth and sampling height. The maximum reduction of volume is seen to be only 27 % for $d_c = 2.5$ in. and $\theta = 0^\circ$.

Comparison With Experimental Results

In Fig. 4.2 the experimental results of volume per unit area for a sampling radius out to 30 in. at a charge depth of 4.5 in., a sampling height of 20.5 in. and sampling terminated at 12 and 17 msec is compared with the constant sample volume calculated from Eq. 7. Sample volumes at

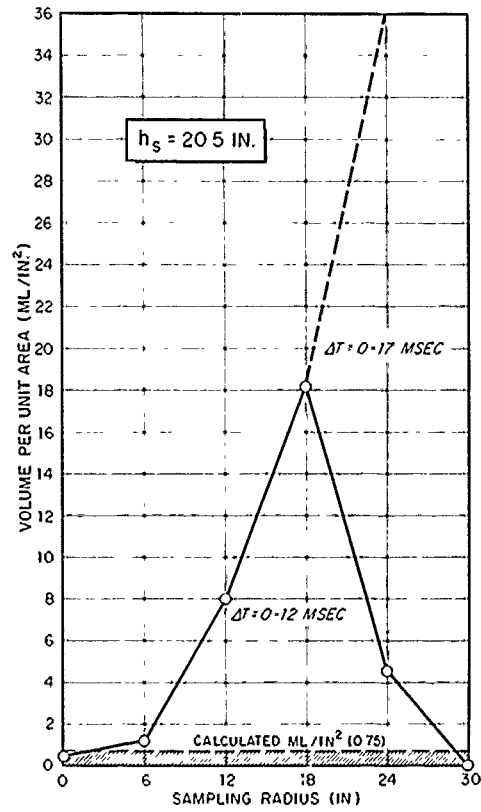


Fig. 4.2 Actual and Calculated Sample to Volume vs Radius for 4.5-in. Charge Depth

these early termination times were used because only the water seal will have passed the samplers. Figure 3.2 shows no volume increases until after 102 msec except a minor change at the 6 in. radius. At the center the volume per unit area sampled is in good agreement with the calculated volume per unit area, but measured volume increases sharply over calculated volumes with increasing sample radius up to 18-in. The sample volume then drops to zero simply because the initial expansion of the bubble is not completed. Pictures show that at 12 msec, the sampler at 30 in. radius is just outside the column. Also note that nearly all the volume at sample radius of 24 in. was collected during the 12-17 msec time period as indicated on Fig. 4.2.

This figure clearly shows that the assumption of radial flow which resulted in calculation of constant volume per unit area for all sampling radii is not correct except at the center axis.

To see how well the radial-flow assumption described the seal thickness over the charge depths of interest, the seal thickness on the center axis at a height of 20.5 in., as given by Eq. 5 is compared with the seal thickness calculated from early sampling data in Fig. 4.3. The experimental seal thickness is calculated by dividing the sampling volume by the effective area of the sampler. Table 4.1 gives the tabulated values of seal thickness and sample termination times. From Fig. 4.3 it is seen that seal thickness given by sampling data is less than the calculated values for charge depths less than about 5 in., but variation is not significant because the sample volumes are less than 1 ml, which approaches the resolution of sample-volume measurements. At charge depths of 12 and 24 in., the sampling data indicate seal thicknesses a factor of two more than calculated values. Thus, the seal thickness as calculated from the radial-flow assumption cannot account for the observed seal thickness at the column center axis. The most likely

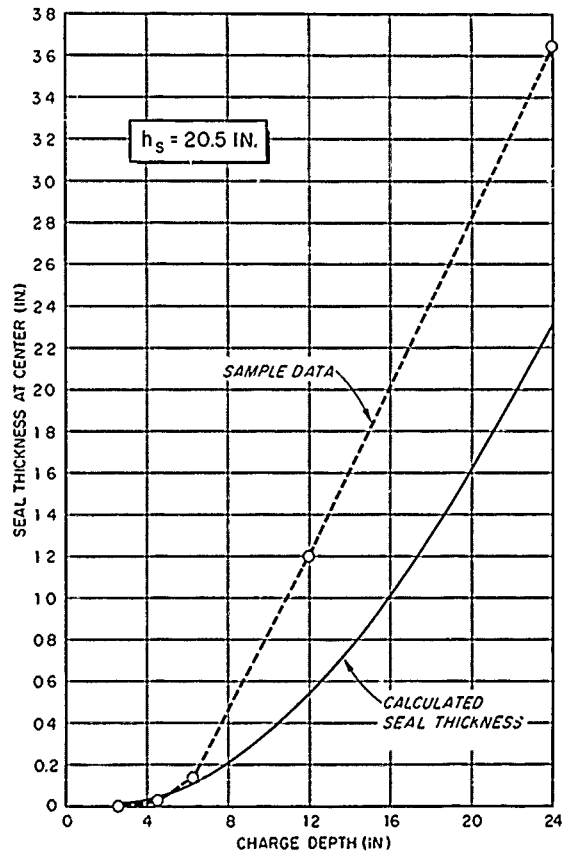


Fig. 4.3 Actual and Calculated Seal Thickness vs Charge Depth

TABLE 4.1

Charge Depth (in.)	Sample Volume (ml)	Termination Time (msec)	Seal Thickness (in.)
2.5	0	12	0
4.5	0.2	17	0.03
6.3	1.0	17	0.14
12	8.7	22	1.2
24	26.3	32	3.65

explanation for this is that the sample termination time was late enough to include additional sample volume due to the converging tangential flow in the expanding seal. The sample termination times for the 12 and 24-in. charge depths were 22 and 32 msec respectively, while times for the shallower depths were 12 or 17 msec. This implies that convergence occurs quite early at these charge depths. Convergence may also occur equally early for the shallower charge depths considered, but at a level above the 20.5-in. sampling height.

Total Ejected Water Calculation

Just as sample volumes are readily calculated with the assumption that water lying initially over the charge flows only radially, total ejected water volume may similarly be calculated. With only radial flow, the total ejected water will be the difference between (1) the volume of water in a cone with its point at the charge center, its base at the water surface and its revolved side a line from the charge center to the maximum sample radius, and (2) the volume of the included sector of the charge. An equation for the total ejected volume may readily be derived by subtraction of the charge sector volume from the cone volume

with all dimensions in convenient notation. The resulting equation with the ejected volume in liters is:

$$V_t = \frac{\pi}{183} (r_s/D)^2 d_c^3 - \frac{2\pi r_o^3}{183} (1 - D/(D^2 + r_s^2)^{1/2})$$

where $D = d_c + h_s$, d_c is charge depth, h_s is sampling height, r_s is sampling radius, and r_o is the charge radius. This is not a general equation. The values of h_s , r_s and d_c must be selected for a realistic case.

In Fig. 4.4 the total ejected water volume, as calculated from the above equation with a sampling height of 20.5 in. and a sampling radius of 42-in. has been plotted for charge depths of 2.5 to 24-in. For comparison, volumes calculated from sampling data presented in Table 3.1 are plotted with associated time intervals. It can be seen that all values of total ejected water are greater than those of the volume calculated from the equation except for one at a charge depth of 24 in. Actually, values for time intervals of less than 50 msec at any charge depth do not represent the actual total volume because the column has not as yet reached the 42-in. sampling radius assumed for the volume calculation. In spite of this consideration, ejected water volumes for early time intervals up to charge depths of 12 in. lie well above the calculated volumes. Since the ejected water volume was calculated with the assumption of pure radial flow and definitely does not correlate with the ejected water volume from sampling data, it must be concluded that flow in the water seal consists of an additional non-radial, or tangential, component. This additional water must be supplied from the area surrounding the bubble, but its specific source is not clearly apparent as yet.

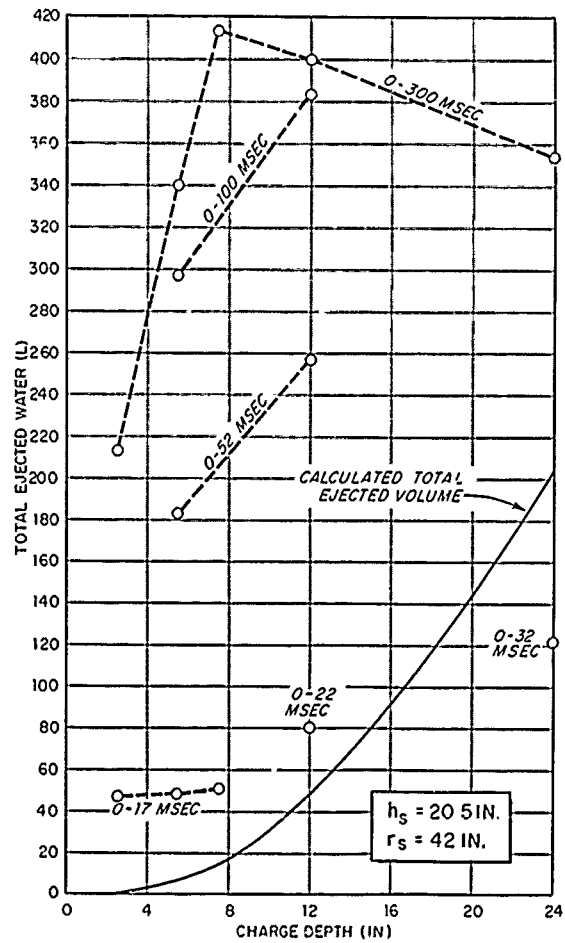


Fig. 4.4 Actual and Calculated Total Projected Water vs Charge Depth

Internal Structure

Time Sequence of Column Structure

With detailed sampling data for the 5.5- and 12-in. charge depths, and photographic results from previous Hydra program projects,⁴ it is now possible to construct an approximate time sequence of the column development. Since the underwater bubble is intimately associated with the column, it must be included in any structural picture; however, only such shape and gross-flow data as are apparent from underwater pictures will be included.

Two series of sectional drawings of the column and bubble for progressive times through the event are presented in Figs. 4.5 and 4.6 for charge depths of 5.5 and 12 in., respectively. Each series of drawings diagrams an event in the following manner. The event is divided into specific times when sampling data and outline drawings from motion-picture records of the column and bubble were both available. The sample volumes for each interval are indicated by solid vertical arrows of length roughly proportional to the sample volume and located at the proper height and radius. The time intervals when the samples were obtained are indicated at the right side of the black sampling arrows and when possible, cover only the time interval between drawings. Sampling at the 6-ft height was never terminated before 100 msec and is presented on the 100-msec drawing but represents sampling from zero time. The patterns of flow within the column, deduced from the preceding information, are represented by dashed arrows. A dashed line (long dashes) represents what is apparently an interior column boundary that conflicted, in construction of the diagram, with the column outline. The area outside the dashed line must consist of very low-density spray.

Considerations taken into account in the construction of each interval of Fig. 4.5 were as follows:

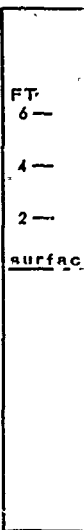
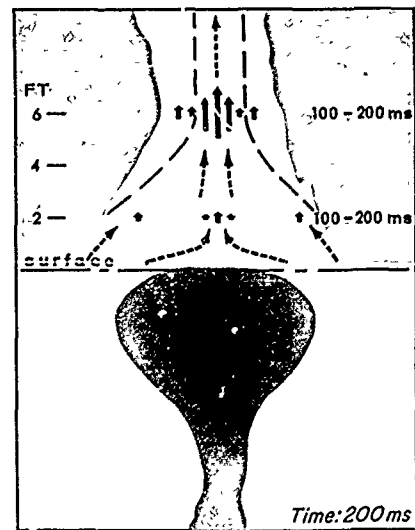
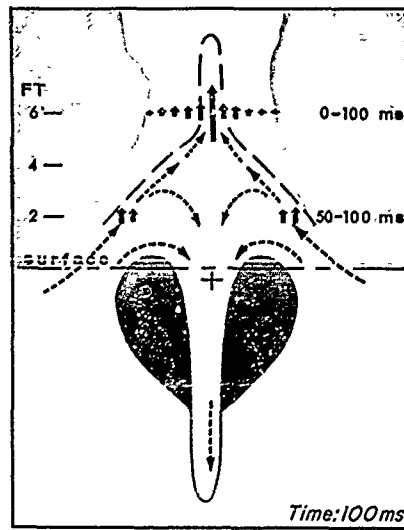
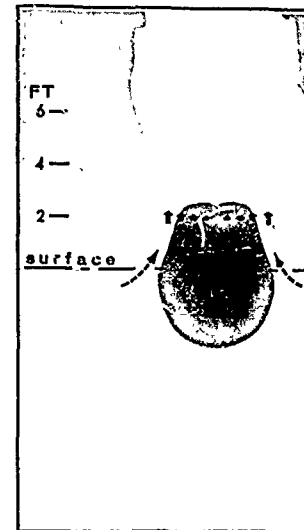
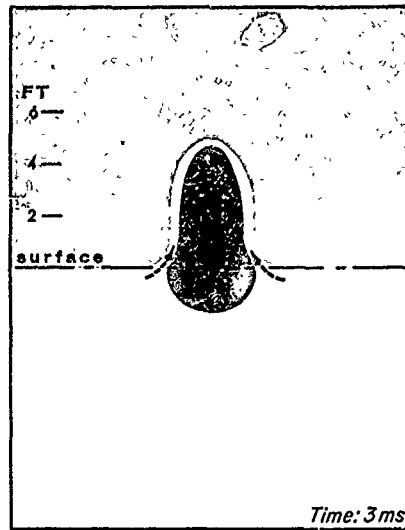
Time = 3 msec. Here the column is in the initial stages of expansion and may be reasonably described by pure radial flow; however, tangential flow may be starting.

Time = 10 msec. The first results of sampling at 2 ft show an increase in water volume collected with radius which indicates that tangential flow is well established as is indicated by dashed arrows. The height and shape of the bubble above the surface are uncertain, but it is very likely that the water seal has broken and that the explosion products have started to blow out. This process will continue until the internal gas pressure drops below atmospheric.

Time = 50 msec. Now, samples only at the outer radius of the 2-ft level and the appearance of the downward jet from the bottom of the bubble dictate that the tangential flow has split. Assurance that an upward jet has also formed requires the reader to look ahead to the 100 msec drawing where a large sample at the 6-ft level is evident.

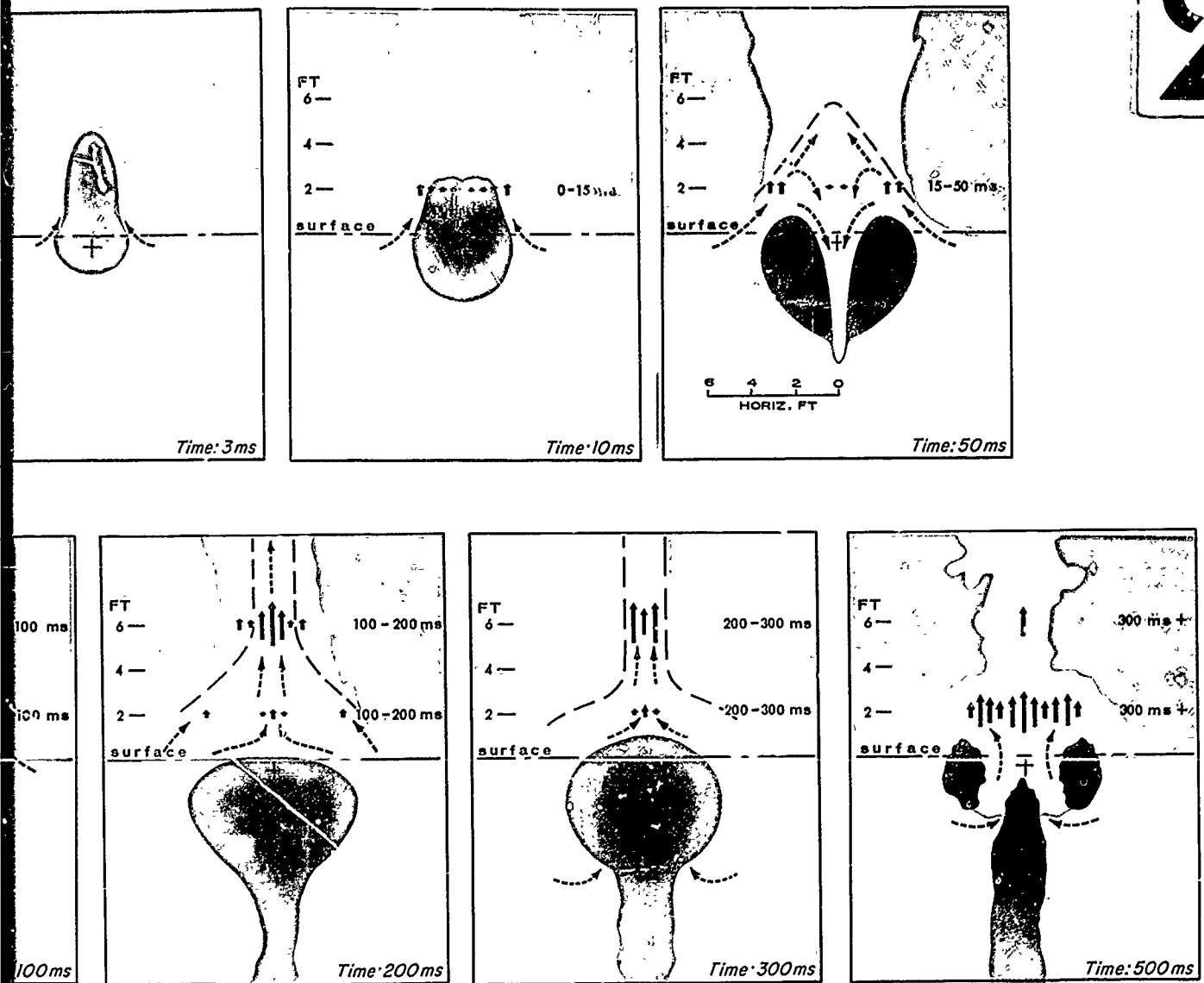
Time = 100 msec. No basic change in flow pattern is evident. The samples at the 6-ft level for the first 100 msec are presented and, considering the moderately large sample volumes at radii of 5 and 12 in., the original convergence probably occurred at 6 ft.

Consideration of total ejected water volume given in Fig. 3.13 for sample heights of 2 and 6 ft at this interval reveals that a large part of the water passing upward through the 2-ft sampling level does not pass through the 6-ft level even at later times. If this large volume does not continue upward, it must be deflected into the downward jet which pierces the bubble (indicated by the curved arrows). The portion of convergent water flow passing through the 2-ft level at a sampling radius of 36 to 42 in. and continuing to the center at the 6-ft level should be evident at the 4-ft level with a sample radius of about 2 ft.

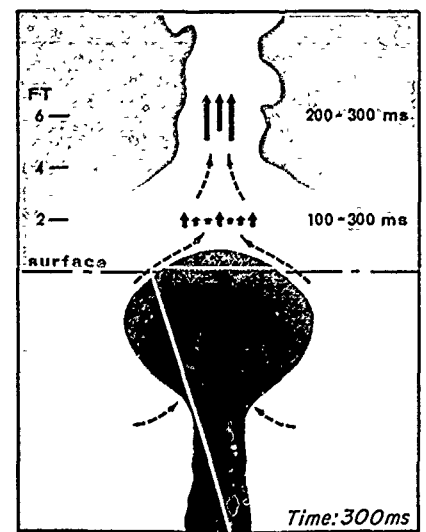
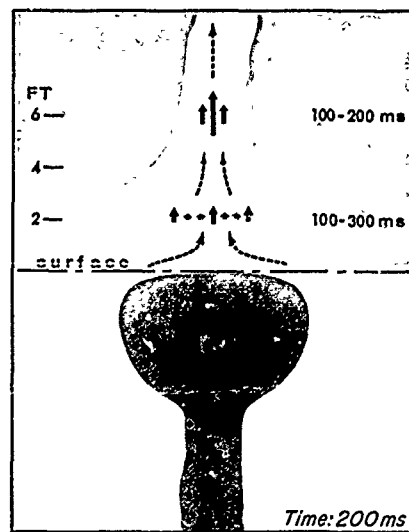
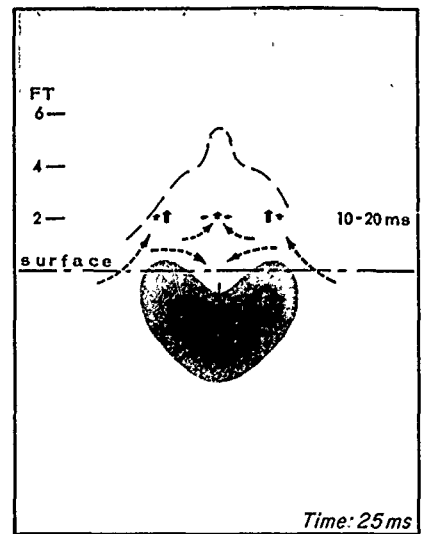
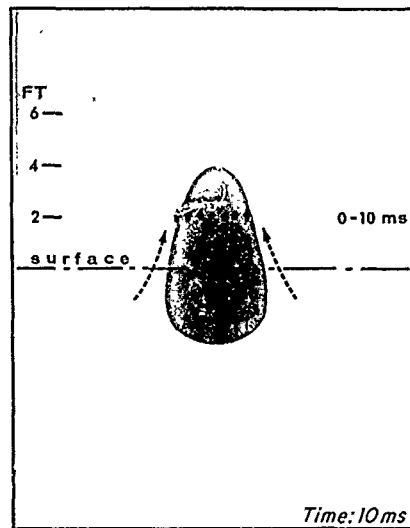


1

Fig. 4.5 Time Sequence of Bubble and Column Internal



g. 4.5 Time Sequence of Bubble and Column Internal Structure for 5.5 in. Charge Depth



1

Fig. 4.6 Time Sequence of Bubble and Column Inter

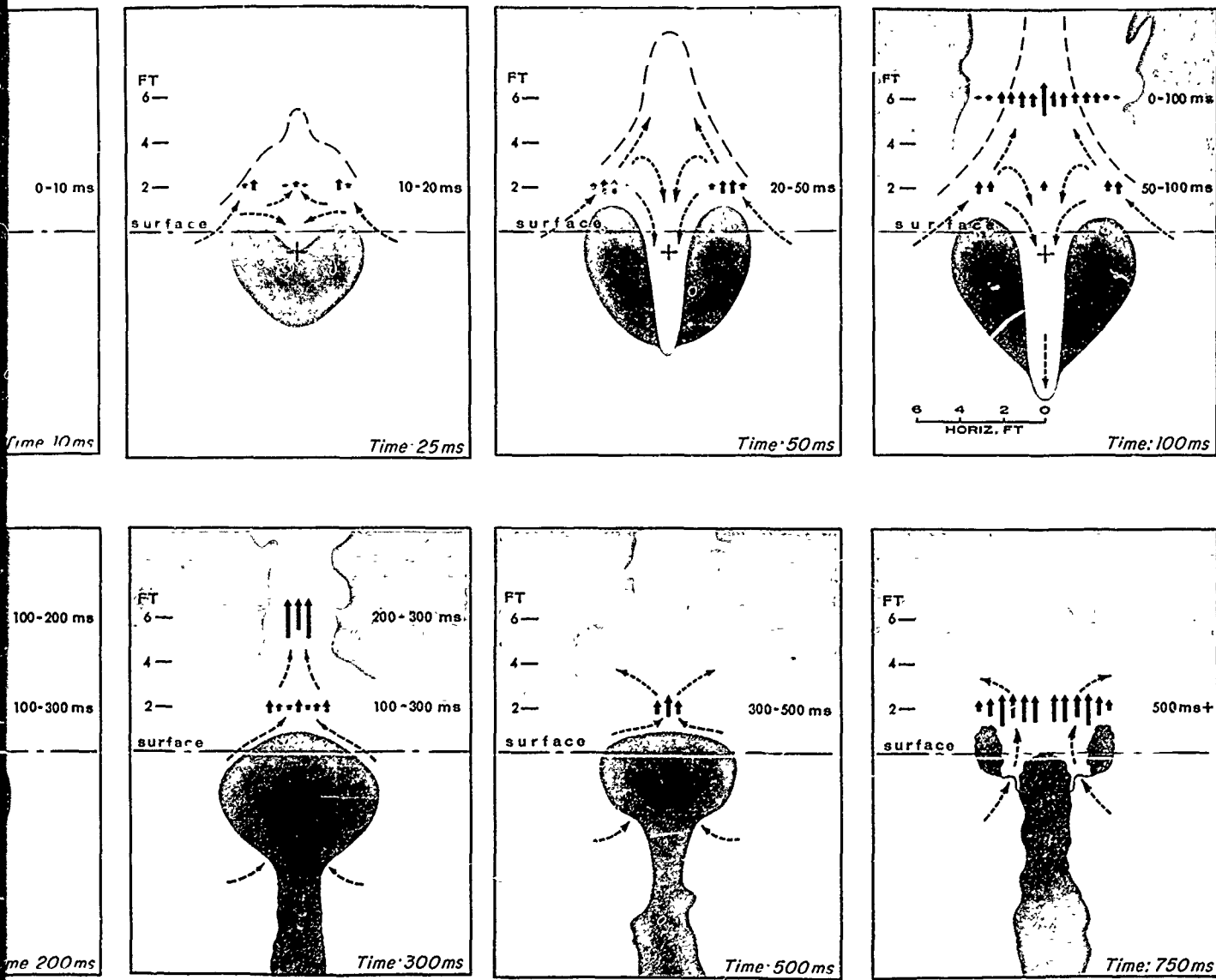


Fig. 4.6 Time Sequence of Bubble and Column Internal Structure for 12 in. Charge Depth

This prediction is indeed supported by a peak in the total sample height of 4 ft as shown in Fig. 3.11. Also the ejected water for the total event as given in Table 3.1 is nearly equal for all sampling heights above 2 ft.

Time = 200 msec. The downward jet is seen to have ceased while the top of the bubble has moved downward. Flow is continuing at both sampling levels and Fig. 3.13 indicates that the total ejected water passing through the 6-ft level exceeds that passing through the 2-ft level during the 100-200 msec time interval.

Time = 300 msec. Flow now is limited to the center only, and the higher volume collected at the 6-ft height may be water which passed through the 2-ft sampling height during the previous interval as shown by the arrows near the periphery on previous views. Note that the bubble has moved upward and shows signs of collapse from the bottom.

Time = 500 msec. The bottom collapse is now underway and the resulting samples from 300 msec to the end of the event are indicated. Almost no water reaches the 6-ft level during this period. Details of the process through which the bubble finally vents by collapsing from the bottom upward are not clear. However, the drawing represents the most plausible method consistent with underwater pictures.

The sequence of events for the 12-in. charge depth as shown in Fig. 4.6 is much the same except for a somewhat later final venting of the bubble.

Carbon in Samples

Results from Chapter 3 show carbon to be present in samples at the 2-ft sampling height at radii of 6 and 12 in. for the earliest sampling time (12-17 msec) at all charge depths to 12 in. If it is assumed that carbon would be found only in samples where the sampler

protruded into the initially expanding bubble, it must be concluded that the horizontal diameter of the bubble at 2 ft above the surface is approximately 2 ft. Carbon was not observed at sampling radii greater than 1 ft at 2 ft above surface at any later time during the event. It is possible to hypothesize that the initial bubble expanded vertically to the 6-ft sampling level while retaining its 2-ft cylindrical diameter, since carbon was also observed during the first time interval of 100 msec. Because upward jetting had already begun, it is more probable that the carbon was picked up at a lower level by the converging tangential flow and included in the jet. Sampling at early times at heights slightly below the convergence level (about 6 ft) should provide the required information to determine the height of initial bubble expansion. Carbon also is observed at several locations in the column which are well removed from the explosion-product bubble at any time during the event, so it must be concluded that the carbon was picked up by the water during interaction with the explosion products occurring earlier in the event.

The dry carbon samples at a sample height of 2 ft for the 2.5 in. charge depth may indicate the predicted "blow-out" of the water seal for this scaled charge depth.⁵

CHAPTER 5

CONCLUSIONS

A reasonably complete description of the internal structure of the column for shallow one-pound explosions has been presented. It is seen that true radial flow outward from the charge center occurs only during the very early initial bubble expansion and is soon supplemented by a tangential flow that results in convergence of the water well above the surface. The convergence results in both an upward jet which rises high into the air and a downward jet which protrudes through the underwater bubble before it reaches maximum diameter. This phenomena is best described as being similar to the case of two co-axial impinging jets and the resulting symmetrical radial flow skirt but with the flow directions reversed. Of the total volume of water involved in the tangential flow, approximately half goes to the upward and half to the downward jet. Convergent flow with upward jetting continues after the downward jet has ceased, but with diminishing quantity and velocity. Final venting of the bubble containing the explosion products occurs when the bubble collapses from the bottom upward.

Clearly, any theoretical bubble model which depends on a radial flow constraint will not predict the exact above surface effects for shallow one-pound underwater detonations, except for very shallow depths and during the very early period of bubble expansion. Both the shape of the predicted above-surface column and the volume of water included are seen to be incorrect.

The question now arises regarding the application of this structural description to larger HE and nuclear yields. If a convergent tangential flow and a downward jet are prominent features of the column resulting from shallow nuclear underwater weapons, they will have several effects on the surrounding radiation-field history. Briefly, these would be the increased attenuation of the field due to the relatively thick column walls or seal, containment of the fission products in the lower portion of the column, and removal of fission products from the bubble to adjacent water by a downward jet.

The converging flow phenomena has been observed previously during small scale vacuum tank studies of shot Baker.^{7,8} Here atmospheric pressure above the water surface was the controlling variable with abrupt convergence into a jet at one atmosphere changing into a straight-sided Baker column at reduced pressures. When speculating as to whether or not the walls of the Baker column did converge, the authors of the above references do not agree. The major significance of extrapolating these results to the nuclear case is that convergence may well act as a containment mechanism that limits the blowout of fission products partially or completely. The most accepted picture of "blowout" has the fission or explosion products contained by the expanding seal of water above the surface until conditions of surface roughness and pressure differential result in an unstable condition in which the seal can no longer contain the fission products and blowout occurs. If expansion of the bubble has progressed to the point where its pressure is below atmospheric, "blowin" will occur when the seal becomes unstable. A more complex picture of blowout, which includes convergence is as follows: the layer of water above the charge moves upward radially forming a water seal which contains the explosion or fission products; however, simultaneously water is flowing into the seal tangentially. For the blowout condition, the seal at the central axis, which is moving upward at high velocity, thins

and soon becomes unstable; thereby allowing the explosion products to escape. The thick portion of the seal where tangential flow has dominated soon converges at the center axis and again seals off the explosion products. For the non-blowout case, the tangential flow converges before the seal breaks at the center; thereby containing the explosion products in the lower portion of the column. Assuming that the radial velocity of the original water seal and the time of convergence are dependent on charge depth, it is expected that there is a critical depth for each explosive yield where no blowout occurs, and an increasing degree of blowout for shallower depths. Experimental determination of the internal column structure of large nuclear weapons is not feasible, but external measurements may be more readily explained in view of the possible internal structure described here.

REFERENCES

1. D. T. Goertner. Vacuum Tank Studies of Underwater Explosion Bubbles Scaled to the Nuclear Range. NAVORD Report No. 3714, April 1954.
2. Classified document.*
3. Classified document.*
4. J. W. Hendricks, D. L. Smith. Above and Below Surface Effects of One-Pound Underwater Explosion, HYDRA I. U. S. Naval Radiological Defense Laboratory Technical Report, USNRDL TR-480, 18 October 1960.
5. J. G. O'Connor, Jr., D. E. Phillips. A Gage for Investigating the Internal Structure of the Columns Produced by Shallow Underwater Explosions". Navy Ordnance Laboratory TR-61-111, 13 September 1961.
6. Classified document.*
7. Classified document.*
8. Classified document.*

*For a list of the classified references, interested readers should write to the author.

APPENDIX

TABULATION OF SAMPLING DATA

$d_c = 2.5$ in.

$h_s = 20.5$ in.

R (in.)	Termination Times	Number Samples	Cumulative Sample Volume (ml)			Remarks
			Max.	Min.	Ave.	
0	12-17-27	4	0	0	0	
0	300	1	-	-	52	
0	"	2	66	54	60	
6	12-17-27	8	T	0	0	
6	300	2	12	8	10	
6	"	4	43	20	38.6	6 ml sample deleted
12	12-17-27-300	10	T	0	0.5	
12	"	4	6	T	2.3	43 ml sample deleted
18	12-17-27	8	8.5	5.5	6.8	
18	300	2	8	8	8	
18	"	4	21.5	6.5	13.8	125 ml sample deleted
24	12	2	T	0	0.25	
24	17-27	6	21	16.5	18.5	
24	300	2	21	21	21	
24	"	4	75	24	54	153 ml sample deleted
30	12-17-27	8	T	0	0	
30	300	2	29.5	27	28.3	
30	"	4	50	29	38.0	
36	12-17-27	7	0	0	0	
36	300	2	27.5	22	24.7	
36	"	4	65	42	57.0	
42	12-17-27	8	0	0	0	
42	300	2	T	T	0.5	
42	"	4	2.5	T	1.3	

NOTE: "T" indicates trace, or a volume of less than one ml. A value of 0.5 ml has been used when averaging with other values.

$$d_c = 2.5 \text{ in.}$$

$$h_s = 68.5 \text{ in.}$$

R (in.)	Termination Times	Number Samples	Cumulative Sample Volume (ml)			Remarks
			Max.	Min.	Ave.	
0	300, ∞	2	418	262	340	
6	300	4	156	54	62.7	
12	300	4	27	7	12.6	
18	300	4	5	3	4.0	
24	300	4	3	T	1.8	
30	300	4	T	T	0.5	
36	300	4	T	0	0.1	
42	300	4	0	0	0.0	

$$d_c = 5.5 \text{ in.}$$

$$h_s = 20.5 \text{ in.}$$

0	12,17,52,102	8	2.5	0	0.2	
0	200	2	11.5	11.5	11.5	
0	300	3	43.5	7.0	26.5	
0	500,700,∞	6	123.0	59.0	110.0	
6	12,17	4	1.0	T	0.5	
6	52,102	6	4	1	2.5	
6	200	4	10	4	6.6	
6	300	6	26	1	13.2	
6	500	2	52	34	43.0	
6	700,∞	10	76	41	65.0	
12	12,17,52,102	22	7.5	1	3.5	
	200,300					
12	500	2	7	5	6.0	
12	700	2	27	17	22.0	
12	∞	6	111	4.5	27.6	
18	12,17,52, 102,200,300	22	14.5	3	8.0	34 ml sample deleted

Continued

R (in.)	Termination Times	Number Samples	Cumulative Sample Volume (ml)			Remarks
			Max.	Min.	Ave.	
18	500,700	4	14	9	11.0	
18	∞	6	138	9	44.3	
24	12	2	4	T	2.2	
24	17,52,102, 200,300	19	20	11.5	15.5	
24	500,700	4	26	14.5	20.0	
24	∞	6	154	18	80.8	
30	12,17	4	0	0	0	
30	52,102,200, 300,500,700	19	29	20	26.0	
30	∞	6	107	25	50.0	
36	12,17	5	T	0	0	
36	52	2	23	20	21.5	
36	102,200,300 500,700,∞	24	40	25	30.0	2 ml sample deleted
42	12,17,42	6	0	0	0	
42	102	4	34.5	16.5	22.6	
42	200,300,500 700,∞	21	59	3	32.0	

NOTE: Shots at termination times of 12 and 17 msec were fired at $d_c = 4.5$ in.

$d_c = 5.5$ in.

$h_s = 68.5$ in.

0	100	1	-	-	142.5
0	200	1	-	-	245.0
0	300	1	-	-	280.0
0	∞	1	-	-	330.0
6	100	2	13.5	11.5	12.5
6	200	2	67.5	66.0	66.8
6	300,∞	4	158.0	133.0	148.0
12	100	2	7.5	7.0	7.3
12	200,300,∞	6	22	9	15.2
18	100	2	6	5	5.5

Continued

R (in.)	Termina- tion Times	Number Samples	Cumulative Sample Volume (ml)			Remarks
			Max.	Min.	Ave.	
18	200,300,∞	6	15.5	5.5	9.1	
24	100,200,300,∞	8	9	4	6.8	
30	100,200,300,∞	8	6	1.5	3.6	
36	100,200,300,∞	8	1.5	T	0.5	
42	100,200,300,∞	8	T	0	0.2	
d _c = 5.5 in.						
h _s = 44.5 in.						
0	∞	1	-	-	125	
6	∞	2	92	41	66.5	
12	∞	2	3	T	1.8	
18	∞	2	6.5	5.5	6.0	
24	∞	2	37	34	35.5	
30	∞	2	8	6.5	7.3	
36	∞	2	T	T	0.5	
42	∞	2	0	0	0	
d _c = 5.5 in.						
h _s = 92.5 in.						
0	∞	1	-	-	343	
6	∞	2	190	138	164	
12	∞	2	31	7	19	
18	∞	2	9.5	5	7.3	
24	∞	2	6	3	4.5	
30	∞	2	4	1	2.5	
36	∞	2	T	T	0.5	
42	∞	2	0	0	0	

$d_c = 7.5$ in.

$h_s = 20.5$ in.

R (in.)	Termination Times	Number Samples	Cumulative Sample Volume (ml)			Remarks
			Max.	Min.	Ave.	
0	17	3	2.5	T	1.0	
0	300	1	-	-	75	
0	∞	1	-	-	124	
6	17	6	4	1	2.3	
6	300	2	40.5	18.5	10.8	
6	∞	2	114	76	95	
12	17	6	3.5	2	2.5	
12	300	2	11.5	10	10.8	
12	∞	2	59	8	33.5	
18	17	6	12	5	8.8	
18	300	2	14	13	13.5	
18	∞	2	17	11	14	
24	17	6	22	15	17.3	
24	300	2	18.5	17.5	18	
24	∞	2	126	27	76.5	
30	17	2	0	0	0	
30	300	2	28	26	27	
30	∞	2	103	52	77.5	
36	17	4	0	0	0	
36	300, ∞	4	31.5	26.5	29.4	
42	17	6	0	0	0	
42	300	2	45.5	36	40.8	
42	∞	2	56	51	53.5	

Actual depth for all shots terminated at 17 msec is $d_c = 6.3$ in.

$d_c = 7.5$ in.

$h_s = 68.5$ in.

R (in.)	Termination Times	Number Samples	Cumulative Sample Volume (ml)			Remarks
			Max.	Min.	Ave.	
0	300	1	-	-	299	
0	∞	1	-	-	356	
6	300	2	236	212	224	
6	∞	2	317	238	278	
12	300, ∞	4	27.5	14	17.5	
18	300, ∞	4	12.5	11	11.1	
24	300, ∞	4	11	7	9	
30	300, ∞	4	3.5	1.5	2.4	
36	300, ∞	4	T	T	0.5	
42	300, ∞	4	0	0	0	

$d_c = 12$ in.

$h_s = 20.5$ in.

0	22,52	3	9	8.5	8.8	
0	102	1	-	-	18.5	
0	300	1	-	-	361	
0	500, ∞	3	120	63	89.5	
6	22,52,102	8	15	9	10.7	
6	300	2	21.5	8	14.8	
6	500	2	66	30	4.8	
6	∞	4	134	44	107	
12	22,52,102	8	11	8	9.5	
12	300,500	4	23.5	11.5	14	
12	∞	4	115	23	70.3	
18	22,52,102	8	17	11.5	14.3	
18	300,500	4	33.5	13.5	19.1	
18	∞	4	143	48	72.5	
24	22	3	18	16.5	17.3	
24	52,102,300,500	8	32.5	14	23	
24	∞	4	178	39	92	
30	22	4	3.5	2	2.8	

Continued

R (in.)	Termination Times	Number Samples	Cumulative Sample Volume (ml)			Remarks
			Max.	Min.	Ave.	
30	52,102,300, 500	8	30	23.5	26	
30	∞	4	118	48	83	
36	2.2	4	0	0	0	
30	52	2	27	26	26.5	
36	102,300,500, ∞	10	67	30	44	
42	22	4	0	0	0	
42	52	2	13	T	6.7	
42	102	2	35	19	27	
42	300,500,∞	8	67	20	48	
$d_c = 12$ in.						
$h_s = 68.5$ in.						
0	100	1	-	-	76	
0	200	1	-	-	204	
0	300,∞	4	394	214	304	
6	100	2	32	16.5	24.3	
6	200	2	64	41	52.2	
6	300,∞	7	263	122	180	23 ml sample deleted
12	100,200, 300,∞	12	40	14	25	
18	100,200,300,∞	12	28	14.5	22	
24	100,200,300,∞	12	26	12	18	
30	100,200,300,∞	12	16	1	11	
36	100,200,300,∞	12	17	T	8.3	
42	100,200,300,∞	9	10	0	3.1	Three 0 ml samples deleted
$d_c = 12$ in.						
$h_s = 44.5$ in.						
0	∞	1	-	-	24.5	
6	∞	2	11	4.5	7.8	
12	∞	2	2.5	2.5	2.5	
18	∞	2	7.5	5	6.8	
24	∞	2	22.5	17	19.8	
30	∞	2	37	27	34	
36	∞	2	23.5	8.5	16	
42	∞	2	18	1.5	9.3	

$d_c = 24$ in.

$h_s = 20.5$ in.

R (in.)	Termination Times	Number Samples	Cumulative Sample Volume (ml)			Remarks
			Max.	Min.	Ave.	
0	30	3	28	25	26.3	
0	300	1	-	-	94	
0	∞	1	-	-	110	
6	30,300	8	34	19	28	
6	∞	2	55	29	42	
12	30,300	8	39	23	33	
12	∞	2	128	48	88	
18	30,300	8	32.5	22	27	
18	∞	2	105	83	94	
24	30	6	18	11	14.2	
24	300	2	31.5	23.5	27.5	
24	∞	2	137	50	93.5	
30	30	6	2.5	T	0.8	
30	300	2	27.5	21	24.3	
30	∞	2	45.5	19	32.3	
36	30	6	0	0	0	
36	300, ∞	4	2.8	22	24.8	
42	30	6	0	0	0	
42	300, ∞	4	23.5	10	19	

$d_c = 24$ in.

$h_s = 68.5$ in.

0	300	1	-	-	245	
0	∞	1	-	-	435	
6	300	2	2.55	235	245	
6	∞	2	314	251	283	
12	300, ∞	4	77	35.5	51.8	
18	300, ∞	4	60	15	32.2	
24	300, ∞	4	22	8	15.5	
30	300, ∞	4	10	4.5	6.9	
36	300, ∞	4	7.5	1	4.8	
42	300, ∞	4	3.5	T	2.0	

DASA-HYDRA IIA DIST.

INITIAL DISTRIBUTION

NO.
CPY

NAVY

1 CHIEF, BUREAU OF SHIPS (CODE 320)
3 CHIEF, BUREAU OF SHIPS (CODE 210L)
1 CHIEF, BUREAU OF SHIPS (CODE 364A)
1 CHIEF, BUREAU OF SHIPS (CODE 423)
1 CHIEF, BUREAU OF NAVAL WEAPONS (RRMA-11)
1 CHIEF, BUREAU OF NAVAL WEAPONS (RR2-5)
2 CHIEF, BUREAU OF YARDS AND DOCKS (CODE 42.330)
1 CHIEF, BUREAU OF YARDS AND DOCKS (CODE 50)
1 DIR. BUREAU OF YARDS -DOCKS (NORTHWEST DIV)
1 CHIEF OF NAVAL OPERATIONS (OP-07T)
1 CHIEF OF NAVAL OPERATIONS (OP-446)
1 OFFICE OF THE CHIEF OF NAVAL OPERATIONS (OP-75)
1 DIRECTOR, NAVAL RESEARCH LABORATORY (CODE 2021)
1 CHIEF OF NAVAL RESEARCH (CODE 418)
5 CO. OFFICE OF NAVAL RESEARCH, FPO, NEW YORK
1 CO.-US NAVAL CIVIL ENGINEERING LABORATORY
1 CO. NAVAL AIR DEVELOPMENT CENTER
1 COMM. U.S. NAVAL ORDNANCE LAB., WHITE OAK (CODE EU)
1 COMM. U.S. NAVAL ORDNANCE LAB., WHITE OAK (CODE E)
1 COMM. U.S. NAVAL ORDNANCE LAB., WHITE OAK (CODE EA)
1 CDR NAVAL ORDNANCE TEST STATION
1 CO. U.S. NAVY ORDNANCE TEST STATION, PASADENA
1 DIRECTOR, NAVAL WEAPONS LABORATORY, DAHLGREN
1 CO. U.S. NAVAL WEAPONS LAB.
1 CO-DIR. NAVY ELECTRONICS LAB. (CODE 2632C)
1 CO-DIR. NAVY ELECTRONICS LAB. (CODE 2350)
1 CO-DIR. DAVID TAYLOR MODEL BASIN (CODE 775)
1 CO-DIR. DAVID TAYLOR MODEL BASIN (CODE 700)
1 CO. DAVID W TAYLOR MODEL BASIN (UARD, CODE 780)
1 DEP. COMM., OPERATIONAL TEST -EVALUATION FORCE, PAC.
1 COMM. OPERATIONAL TEST-EVALUATION FORCE, ATLANTIC
1 DIRECTOR, ARMED FORCES RADIOBIOLOGY RESEARCH INSTITUTE

ARMY

1 OFFICE OF CHIEF RESEARCH AND DEVELOPMENT (ATOMIC OFFICE)
1 CHIEF OF RESEARCH AND DEVELOPMENT (LIFE SCIENCE DIV)
1 DEPUTY CHIEF OF STAFF FOR MILITARY OPERATIONS (CBR)
1 CHIEF OF ENGINEERS (ENGMC-EB)
1 CHIEF OF ENGINEERS (ENGMC-DE)
1 OFFICE OF CHIEF OF ENGINEERS (ENGCM-Z)
1 CG ARMY MATERIEL COMMAND (AMCRD-DE-NE)
1 CG, BALLISTIC RESEARCH LABORATORIES
1 U S ARMY EDGEWOOD ARSENAL
1 CO U.S. ARMY CBR COMBAT DEV COMMAND FT. MCCLELLAN)
1 COMMANDANT, CHEMICAL CORPS SCHOOLS (LIBRARY)

1 CO, CHEMICAL RESEARCH AND DEVELOPMENT LABORATORIES
 1 COMMANDER, NUCLEAR DEFENSE LABORATORY
 1 COMMANDANT ARMY WAR COLLEGE
 1 DIRECTOR, WALTER REED ARMY INSTITUTE OF RESEARCH
 1 CG, COMBAT DEVELOPMENTS COMMAND (CDCMR-V)
 1 CG, QUARTERMASTER RES AND ENG COMMAND
 1 HQ, DUGWAY PROVING GROUND
 3 THE SURGEON GENERAL (MEDPS-NM)
 1 DIRECTOR, USACDS NUCLEAR GROUP
 1 DIRECTOR, WATERWAYS EXPERIMENT STATION
 1 CG, MUNITIONS COMMAND (PICATINNY ARSENAL)
 2 CO, WATERTOWN ARSENAL
 1 CG, ARMY MISSILE COMMAND (REDSTONE ARSENAL)

AIR FORCE

1 ASSISTANT CHIEF OF STAFF INTELLIGENCE (AFCIN-3B)
 5 CG, AERONAUTICAL SYSTEMS DIVISION (ASAPRD-NS)
 1 DIRECTORATE OF CIVIL ENGINEERING (AFOCE-ES)
 1 DIR. THE RAND CORP. (DR. RAPP)
 1 COMMANDANT, SCHOOL OF AEROSPACE MEDICINE, BROOKS AFB
 1 OFFICE OF THE SURGEON (SUP3.1), STRATEGIC AIR COMMAND
 1 CG SPECIAL WEAPONS CENTER KIRTLAND AFB
 1 DIRECTOR, AIR UNIVERSITY LIBRARY, MAXWELL AFB
 2 COMMANDER, TECHNICAL TRAINING WING, 3415TH TTG
 1 COMMANDER, AIR FORCE CAMBRIDGE RSCH LABS.(CRT)
 1 HQ, AIR FORCE TECHNICAL APPLICATIONS CENTER

OTHER DOD ACTIVITIES

3 CHIEF, DEFENSE ATOMIC SUPPORT AGENCY (DASARA-3)
 3 CHIEF, DEFENSE ATOMIC SUPPORT AGENCY (LIBRARY)
 1 COMMANDER, FC/DASA, SANDIA BASE (FCDV)
 1 COMMANDER, FC/DASA, SANDIA BASE (FCTG5, LIBRARY)
 2 OFFICE OF CIVIL DEFENSE (DIR OF RSCH)
 2 OFFICE OF CIVIL DEFENSE, WASHINGTON
 2 CIVIL DEFENSE UNIT, ARMY LIBRARY
 3 DIRECTOR ADVANCE RESEARCH PROJECTS AGENCY
 20 DEFENSE DOCUMENTATION CENTER

AEC ACTIVITIES AND OTHERS

1 ATOMIC ENERGY COMMISSION (DR. HOOPER)
 1 ATOMIC ENERGY COMMISSION (DR. JOSEPH)
 1 U.S. ATOMIC ENERGY COMMISSION (HOLLISTER)
 1 LOS ALAMOS SCIENTIFIC LABORATORY (LIBRARY)
 1 MICHIGAN STATE UNIVERSITY (TRIFFETT)
 1 RESEARCH ANALYSIS CORPORATION
 1 PRESIDENT, SANDIA CORP. (DR. REED)
 1 PRESIDENT, SANDIA CORP. (MERRITT)
 1 DIR. SCRIPPS INST. OF OCEANOGRAPHY (VAN DORN)
 1 DIR. SCRIPPS INST. OF OCEANOGRAPHY (DR. FOLSOM)
 2 U. OF CALIFORNIA LAWRENCE RADIATION LAB, LIVERMORE
 1 U. OF CALIF. LAWRENCE RADIATION LAB. (DR. SHELTON)
 1 WOODS HOLE OCEANOGRAPHIC INSTITUTE

USNRDL

52

TECHNICAL INFORMATION DIVISION

DISTRIBUTION DATE: 25 March 1964

65

<p>Naval Radiological Defense Laboratory USNRDL-TR-706 (DASA Number 1440) HYDRA PROGRAM. HYDRA IIB SERIES - INVESTIGATION BY WATER SAMPLING OF THE INTERNAL STRUCTURE OF COLUMNS RESULTING FROM SMALL SHALLOW UNDERWATER EXPLO- SIONS by K. W. Kaulum 13 Sept 1963 71 p. tables illus. 8 refs. UNCLASSIFIED</p> <p>The internal structure of the columns from one- pound high-explosive shallow under- water explosions has been investigated by means of water sampling for several shallow charge depths. Water samples (over)</p>	<p>1. Underwater explosions. 2. Explosion effects, Underwater-to-air. I. Kaulum, K. W. II. Title.</p> <p>UNCLASSIFIED</p>
<p>Naval Radiological Defense Laboratory USNRDL-TR-706 (DASA Number 1440) HYDRA PROGRAM. HYDRA IIB SERIES - INVESTIGATION BY WATER SAMPLING OF THE INTERNAL STRUCTURE OF COLUMNS RESULTING FROM SMALL SHALLOW UNDERWATER EXPLO- SIONS by K. W. Kaulum 13 Sept 1963 71 p. tables illus. 8 refs. UNCLASSIFIED</p> <p>The internal structure of the columns from one- pound high-explosive shallow under- water explosions has been investigated by means of water sampling for several shallow charge depths. Water samples (over)</p>	<p>1. Underwater explosions. 2. Explosion effects, Underwater-to-air. I. Kaulum, K. W. II. Title.</p> <p>UNCLASSIFIED</p>

taken at varying times across the column diameter at several heights up to 8 ft are used to compute the thickness of the water seal between the explosion product gas bubble and the air of the initial column formation and the total volume of water ejected into the column. These are compared with computed seal thickness and water volume assuming outward flow of the water over the charge to be only radial in direction. Sampling data is used along with above- and below-surface photographs to construct a time sequence of the column structure for charge depths of 5.5 and 12 in. It is shown that true radial flow of water over the charge occurs only during the very early initial bubble expansion and is soon supplanted by a tangential flow which converges well above the surface. The converging water results in both an upward jet which rises high into the air and a downward jet which penetrates through the underwater bubble.

taken at varying times across the column diameter at several heights up to 8 ft are used to compute the thickness of the water seal between the explosion product gas bubble and the air of the initial column formation and the total volume of water ejected into the column. These are compared with computed seal thickness and water volume assuming outward flow of the water over the charge to be only radial in direction. Sampling data is used along with above- and below-surface photographs to construct a time sequence of the column structure for charge depths of 5.5 and 12 in. It is shown that true radial flow of water over the charge occurs only during the very early initial bubble expansion and is soon supplanted by a tangential flow which converges well above the surface. The converging water results in both an upward jet which rises high into the air and a downward jet which penetrates through the underwater bubble.

UNCLASSIFIED

UNCLASSIFIED

<p>Naval Radiological Defense Laboratory USNRDL-TR-706 (DASA Number 1440) HYDRA PROGRAM. HYDRA IIB SERIES - INVESTIGATION BY WATER SAMPLING OF THE INTERNAL STRUCTURE OF COLUMNS RESULTING FROM SMALL SHALLOW UNDERWATER EXPLO- SIONS by K.W. Kaulum 13 Sept 1963 71 p. tables illus. 8 refs. UNCLASSIFIED</p> <p>The internal structure of the columns from one- pound high-explosive shallow under- water explosions has been investigated by means of water sampling for several shallow charge depths. Water samples (over)</p> <p style="text-align: right;"><u>UNCLASSIFIED</u></p>	<p>1. Underwater explosions. 2. Explosion effects, Underwater-to-air. I. Kaulum, K.W. II. Title.</p>
<p>Naval Radiological Defense Laboratory USNRDL-TR-706 (DASA Number 1440) HYDRA PROGRAM. HYDRA IIB SERIES - INVESTIGATION BY WATER SAMPLING OF THE INTERNAL STRUCTURE OF COLUMNS RESULTING FROM SMALL SHALLOW UNDERWATER EXPLO- SIONS by K.W. Kaulum 13 Sept 1963 71 p. tables illus. 8 refs. UNCLASSIFIED</p> <p>The internal structure of the columns from one- pound high-explosive shallow under- water explosions has been investigated by means of water sampling for several shallow charge depths. Water samples (over)</p> <p style="text-align: right;"><u>UNCLASSIFIED</u></p>	<p>1. Underwater explosions. 2. Explosion effects, Underwater-to-air. I. Kaulum, K.W. II. Title.</p>

taken at varying times across the column diameter at several heights up to 8 ft are used to compute the thickness of the water seal between the explosion product gas bubble and the air of the initial column formation and the total volume of water ejected into the column. These are compared with computed seal thickness and water volume assuming outward flow of the water over the charge to be only radial in direction. Sampling data is used along with above- and below- surface photographs to construct a time sequence of the column structure for charge depths of 5.5 and 12 in. It is shown that true radial flow of water over the charge occurs only during the very early initial bubble expansion and is soon supplanted by a tangential flow which converges well above the surface. The converging water results in both an upward jet which rises high into the air and a downward jet which penetrates through the underwater bubble.

UNCLASSIFIED

taken at varying times across the column diameter at several heights up to 8 ft are used to compute the thickness of the water seal between the explosion product gas bubble and the air of the initial column formation and the total volume of water ejected into the column. These are compared with computed seal thickness and water volume assuming outward flow of the water over the charge to be only radial in direction. Sampling data is used along with above- and below- surface photographs to construct a time sequence of the column structure for charge depths of 5.5 and 12 in. It is shown that true radial flow of water over the charge occurs only during the very early initial bubble expansion and is soon supplanted by a tangential flow which converges well above the surface. The converging water results in both an upward jet which rises high into the air and a downward jet which penetrates through the underwater bubble.

UNCLASSIFIED

<p>Naval Radiological Defense Laboratory USNRDL-TR-706 (DASA Number 1440) HYDRA PROGRAM. HYDRA IIB SERIES - INVESTIGATION BY WATER SAMPLING OF THE INTERNAL STRUCTURE OF COLUMNS RESULTING FROM SMALL SHALLOW UNDERWATER EXPLO- SIONS by K. W. Kaulum 13 Sept 1963 71 p. tables illus. 8 refs. UNCLASSIFIED</p> <p>The internal structure of the columns from one- pound high-explosive shallow under- water explosions has been investigated by means of water sampling for several shallow charge depths. Water samples (over)</p>	<p>1. Underwater explosions. 2. Explosion effects, Underwater-to-air. I. Kaulum, K. W. II. Title.</p> <p>UNCLASSIFIED</p>
<p>Naval Radiological Defense Laboratory USNRDL-TR-706 (DASA Number 1440) HYDRA PROGRAM. HYDRA IIB SERIES - INVESTIGATION BY WATER SAMPLING OF THE INTERNAL STRUCTURE OF COLUMNS RESULTING FROM SMALL SHALLOW UNDERWATER EXPLO- SIONS by K. W. Kaulum 13 Sept 1963 71 p. tables illus. 8 refs. UNCLASSIFIED</p> <p>The internal structure of the columns from one- pound high-explosive shallow under- water explosions has been investigated by means of water sampling for several shallow charge depths. Water samples (over)</p>	<p>1. Underwater explosions. 2. Explosion effects, Underwater-to-air. I. Kaulum, K. W. II. Title.</p> <p>UNCLASSIFIED</p> <p>taken at varying times across the column diameter at several heights up to 8 ft are used to compute the thickness of the water seal between the explosion product gas bubble and the air of the initial column formation and the total volume of water ejected into the column. These are compared with computed seal thickness and water volume assuming outward flow of the water over the charge to be only radial in direction. Sampling data is used along with above- and below- surface photographs to construct a time sequence of the column structure for charge depths of 5.5 and 12 in. It is shown that true radial flow of water over the charge occurs only during the very early initial bubble expansion and is soon supplanted by a tangential flow which converges well above the surface. The converging water results in both an upward jet which rises high into the air and a downward jet which penetrates through the underwater bubble.</p> <p>UNCLASSIFIED</p>

<p>Naval Radiological Defense Laboratory USNRDL-TR-706 (DASA Number 1440) HYDRA PROGRAM. HYDRA IIB SERIES - INVESTIGATION BY WATER SAMPLING OF THE INTERNAL STRUCTURE OF COLUMNS RESULTING FROM SMALL SHALLOW UNDERWATER EXPLO- SIONS by K.W. Kaulum 13 Sept 1963 71 p. tables illus. 8 refs. UNCLASSIFIED</p> <p>The internal structure of the columns from one- pound high-explosive shallow under- water explosions has been investigated by means of water sampling for several shallow charge depths. Water samples (over)</p> <p style="text-align: right;"><u>UNCLASSIFIED</u></p>	<p>1. Underwater explosions. 2. Explosion effects, Underwater-to-air. I. Kaulum, K.W. II. Title.</p> <p>Naval Radiological Defense Laboratory USNRDL-TR-706 (DASA Number 1440) HYDRA PROGRAM. HYDRA IIB SERIES - INVESTIGATION BY WATER SAMPLING OF THE INTERNAL STRUCTURE OF COLUMNS RESULTING FROM SMALL SHALLOW UNDERWATER EXPLO- SIONS by K.W. Kaulum 13 Sept 1963 71 p. tables illus. 8 refs. UNCLASSIFIED</p> <p>The internal structure of the columns from one- pound high-explosive shallow under- water explosions has been investigated by means of water sampling for several shallow charge depths. Water samples (over)</p> <p style="text-align: right;"><u>UNCLASSIFIED</u></p>
<p>taken at varying times across the column diameter at several heights up to 8 ft are used to compute the thickness of the water seal between the explosion product gas bubble and the air of the initial column formation and the total volume of water ejected into the column. These are compared with computed seal thickness and water volume assuming outward flow of the water over the charge to be only radial in direction. Sampling data is used along with above- and below- surface photographs to construct a time sequence of the column structure for charge depths of 5.5 and 12 in. It is shown that true radial flow of water over the charge occurs only during the very early initial bubble expansion and is soon supplanted by a tangential flow which converges well above the surface. The converging water results in both an upward jet which rises high into the air and a downward jet which penetrates through the underwater bubble.</p> <p style="text-align: right;"><u>UNCLASSIFIED</u></p>	<p>taken at varying times across the column diameter at several heights up to 8 ft are used to compute the thickness of the water seal between the explosion product gas bubble and the air of the initial column formation and the total volume of water ejected into the column. These are compared with computed seal thickness and water volume assuming outward flow of the water over the charge to be only radial in direction. Sampling data is used along with above- and below- surface photographs to construct a time sequence of the column structure for charge depths of 5.5 and 12 in. It is shown that true radial flow of water over the charge occurs only during the very early initial bubble expansion and is soon supplanted by a tangential flow which converges well above the surface. The converging water results in both an upward jet which rises high into the air and a downward jet which penetrates through the underwater bubble.</p> <p style="text-align: right;"><u>UNCLASSIFIED</u></p>